Assessing the Effectiveness of Lockdowns and Mask Mandates on Reducing COVID-19 Infections in Essential Worker Populations

by
Pablo A. Lopez Duque

A thesis submitted to the Department of Physics,

College of Natural Sciences and Mathematics

in partial fulfillment of the requirements for the degree of

Master of Science
in Physics

Chair of Committee: Greg Morrison

Committee Member: Gemunu Gunaratne

Committee Member: Kevin Bassler

Committee Member: Carlos Ordonez

Committee Member: Kathryn Anderson

University of Houston
August 2021

DEDICATION/EPIGRAPH

To Eve, my wife, and to my family.

PLD

ACKNOWLEDGMENTS

This work was only possible due to the unceasing guidance and help from many people. Firstly, I want to acknowledge my wife, Eve, for her unconditional support, especially during the first stages of this program. She has provided me with the strength I need: whenever I felt discouraged, she would talk to me and make me believe in my skills. All this work would not have been possible without her by my side. She is truly the rock upon which I am confident to build everything else. I would like to sincerely thank my family as well. My parents have sacrificed a lot for my education, often prioritizing my needs over their own. Their support has been so outstanding, that I will always be indebted to them. My sister has been there for me too, she has been great at keeping my hopes up whenever I was disappointed.

I would also like to acknowledge my advisor, Greg Morrison, for his total support and dedication, his patience during our weekly meetings, and for being an exemplary person. He helped me to understand that having balance between coursework, research and personal life is paramount. I would then like to thank the members of my committee for taking the time reviewing my manuscript and for offering valuable comments and suggestions to improve this work. I am especially grateful with Carlos Ordonez for his timely support and for all the time he dedicated to help me with my career path. it is something that I will cherish for long.

My friends have been another fundamental part during all these years. Their achievements have inspired me to keep pursuing my dreams. Seeing some of them graduate, publishing their first papers and going into professional life, as well as starting their own families have made me conscious on how lucky I have been to be surrounded by such great individuals.

I have been truly "standing on the shoulder of giants". Thank you all for everything you have given to me. I hope to someday repay at least a small piece of what life has granted me with.

ABSTRACT

Throughout history pandemics have been a constant threat for mankind. Still, the COVID-19 disease resulted in the worst health crisis in more than a century. This suggests that more tools are needed to give adequate guidance for decision-making. Several epidemic models have been proposed to understand and forecast the dynamics of spread of infectious diseases. Only a few, however, account for the role of "essential" workers, who must keep interacting face-to-face with others during a pandemic. In this work, we consider how these "essential" workers are disproportionately affected by the pandemic, and how they may act as a reservoir for the disease. We further consider the effect of non-pharmaceutical intervention policies (such as mask mandates and lockdowns), incorporated in a model we term the Local-Policy SIR model. We assume mask mandates are applied only at essential locations, whereas lockdowns function only at non-essential locations.

We find this model suggests mask mandates may not be effective without simultaneous lockdowns as a result of the fast dynamics of non-essential risky workers at early stages of an outbreak. We also find that essential workers may play a fundamental role in the dynamics because they may act as reservoirs of the infection during periods of lockdowns. Our results also suggest that partial lockdowns combined with a high mask mandate compliance may prevent an outbreak. We then investigate the effect of delays in enacting these policies and found that even late implementations benefit the entire population, but the benefit decreases for larger delays. Using a gradient descent algorithm, we extracted the mobility for non-essential workers from active infection curves for New York, Texas, and California. This permits an estimation of the share of each subpopulation in the infection and the hazard ratio of essential vs non-essential workers as a function of time. We show that "essential" workers are likely unfairly affected by the pandemic. The LP-SIR model is also applied to neighborhoods composed of heterogeneous populations. We find evidence that a neighborhood composed mainly of "essential" workers is at disadvantage with respect to a neighborhood composed mainly of "non-essential" workers during an outbreak.

Contents

List of Tables

List of Figures

1 Introduction

Infectious diseases have been a recurring issue in the history of mankind. Examples include outbreaks of the bubonic plague, cholera, HIV, and several types of influenza. Despite the loss of millions of human lives, the tools available to model and forecast their dynamics are still insufficient to contain the spread of the disease or, at least, prevent its adverse effects. A good case in point is the Spanish flu pandemic outbreak in 1918-1919, which was likely caused by a zoonotic infection with the H1N1 virus of avian origins. However, the exact host that introduced it to humans remains unknown [1]. Being a virus that crossed species, the population was caught by surprise. The poor condition of the healthcare system and the unavailability of vaccines exacerbated the consequences of the outbreak. Governmental efforts to contain the spread were constrained to quarantines, social distancing, lockdown policies, mask mandates and similar measures, all of which are known as non-pharmaceutical interventions (NPIs). In spite of this, the death toll of this pandemic was approximately 50 million worldwide [2]. As we emphasize below, this case brings startling similarities with the novel COVID-19 disease, which also resulted in a catastrophic health crisis. The virus which originated the COVID-19 disease seems to have originated in bats [3]. Aside from the zoonotic origin and the unavailability of a vaccine at the beginning of the pandemic, the policy response resembled the response in 1918, with NPIs as the only feasible interventions at the beginning of the outbreak.

In the early 20th century, the world was far less connected than it is today. However, in 1918 (due to World War I), there was a higher than normal mobility that may have contributed to disperse the deadly influenza virus. The 1918 Spanish flu pandemic seems to have originated in the Midwest of the United States, spread to other states and then to Europe [2]. The spread was quick, and the disease had a high attack rate, causing a total of three waves with the last causing most deaths. A peculiar factor of this virus was that it specially targeted healthy adults (< 30 years) [4], instead of older adults or individuals with preconditions, which are commonly hit harder by influenza viruses. Once a wave started, governments tried to limit the spread using simple NPIs to mitigate the transmission. As the most common mode of transportation was by ship, maritime quarantines were put in place in Australia and America Samoa[1]. The decrease in the deaths associated with this pandemic, compared to places where no quarantine was enforced, suggests that fully enforcing timely quarantines limited the casualties. Another policy implemented by some authorities was mask usage. However, due to lack of data it remains unclear if and how masks helped to mitigate the spread. Facemask protection effectiveness depends on several factors, including how and when it is worn, the mask material, and the type of virus causing the disease [1]. For the H1N1 virus, there is some evidence on facemasks protection [5], but for COVID-19 extensive studies have demonstrated their utility. It is clear, though, that low public compliance significantly hinders the effectiveness of facemasks [1]. In the US, a major complication associated to the transmission and analysis of the disease was the wildly varied response from states [6]. Some adopted early social distancing, school closures, and limited gatherings whereas others delayed setting up such policies [7]. Figure 1 shows the wide variation in the outcome for the states of San Francisco, New York, and Philadelphia, with states that had early adoption and more consistent policies less impacted. This story is reminiscent of the COVID-19 pandemic, which originated in China, spread throughout the country, and then to the world. Older adults were highly impacted by this disease. As a response to COVID-19, governments implemented different combinations of NPIs to try to mitigate the transmission. In the US, the most common interventions were recommended social distance, facemask usage, quarantines, and contact tracing. As in the 1918 pandemic, the response on each state within the US varied considerably [8], [9]. The effectiveness of each policy in containing the spread, thus, remains unclear.

As it is clear from the example above, there are several strategies to deal with an infectious disease including prevention, medication, vaccination among other public health measures. Largely, the response depends on the specifics of the virus or bacteria causing the disease. If a vaccine is unavailable, once an outbreak has begun, governments are forced to take quick, untested decisions to try to limit the consequences of the spread. As governments increase awareness and implement

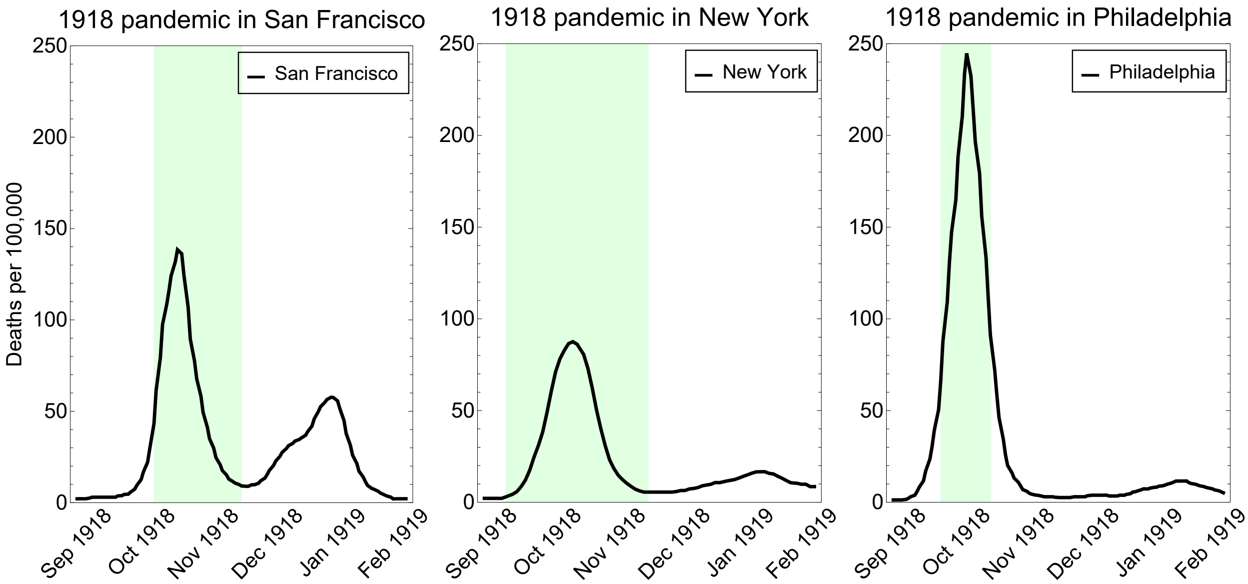

Figure 1: Deaths per 100,000 due to the 1918 pandemic in the US for the states of San Francisco, New York, and Philadelphia. The wide difference in outcomes that results from a distinct set of adopted policies and their timing is shown (NPIs were implemented in the highlighted region). Data was extracted from [6]. Early relaxing or late adoption of policies led to higher excess deaths.

prevention strategies, they must balance important economic consequences of limiting social activities [10], [11] with health risks posed by the disease. Therefore, implementing policies to address and lessen the impact on the population becomes troublesome. Even if the most feasible initial response is through NPIs. It may take a long time from virus first detection to the widespread availability of a vaccine. In the case of COVID-19, even if vaccines are already available, concern remains due to the unknown impact of variants of the virus coupled with a lower than expected rate of vaccination. Thus, it is essential to develop models that can forecast and quantify the consequences of the disease. Specifically, it is important to quantitatively estimate the impact of a given NPI policy to flatten the infection curve and to discern the driving parameters of the disease. That is, to determine under which conditions an outbreak can be avoided or contained.

In 2020, the modern world had to endure the COVID-19 pandemic, one of the worst health crises in more than a century. The SARS-CoV-2 virus, which causes the COVID-19 disease was initially detected in Wuhan, China, at the end of 2019. Due to the globalization of our modern world, the virus swiftly spread throughout Asia, Europe, North America, and the rest of the world. By

March 2020, it had been introduced into most countries, which were largely unprepared. The policy response varied considerably depending on the country and local governments. In some countries, the implemented policies and compliance led to a flatter infection curve, whereas in other locations community spread and reinfections became a common issue. Data for active infections and deaths for a few countries was taken from [12] to exemplify distinct types of outcomes. For instance, in China and Singapore, the COVID-19 disease was contained by May 2020 and October 2020, respectively. Figure 2 shows that, in China, the infection curve had only one peak, with only a minor localized onset after it. Likewise, in Singapore, there was a peak corresponding to the initial infection along with a few contained outbreaks. On the contrary, there are countries that are still

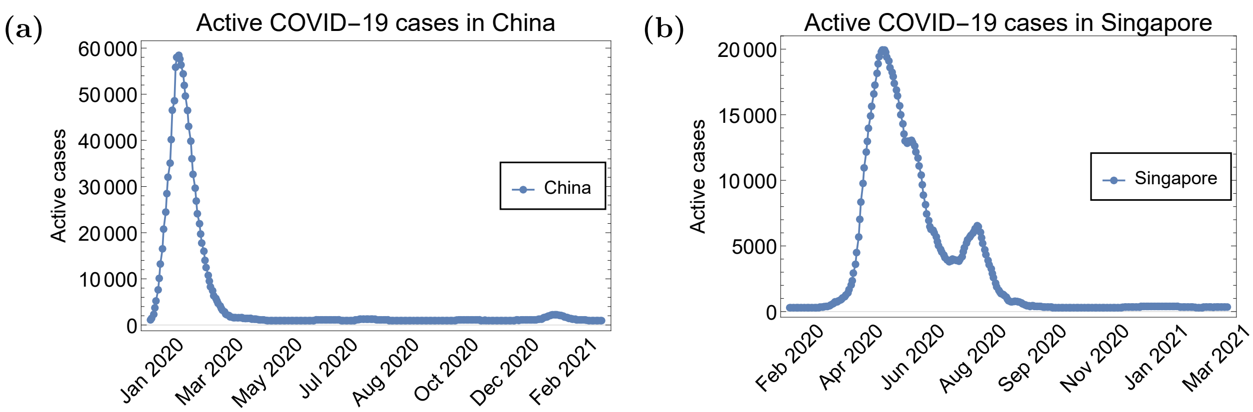

Figure 2: Active infection curves for COVID-19 disease in a) China, b) Singapore, showing the dynamics in countries that adopted a more stringent set of policies. The resulting dynamics show one main peak with a few minor secondary peaks. The infection was controlled relatively quickly and there is no reported sign of a further outbreak. Data taken from [12] .

struggling with the effects of the COVID-19 pandemic, e.g., Brazil, and India, where infections are still high as of this writing. Figure 3 illustrates the active infection curves for these two countries, which show complicated dynamics. This indicates they have struggled to contain the spread. As of April 2021, more than a year after the pandemic began, containment is still a worldwide issue. As it can be seen in Figure 4, the trend is still increasing. By the end of March 2021, the number of total cases in the world was nearly $130,000,000$ and the number of total deaths was approximately $2,840,000$. While the impact of the recently developed COVID-19 vaccine is promising, several communities worldwide have limited access to the vaccine, and within the US many communities

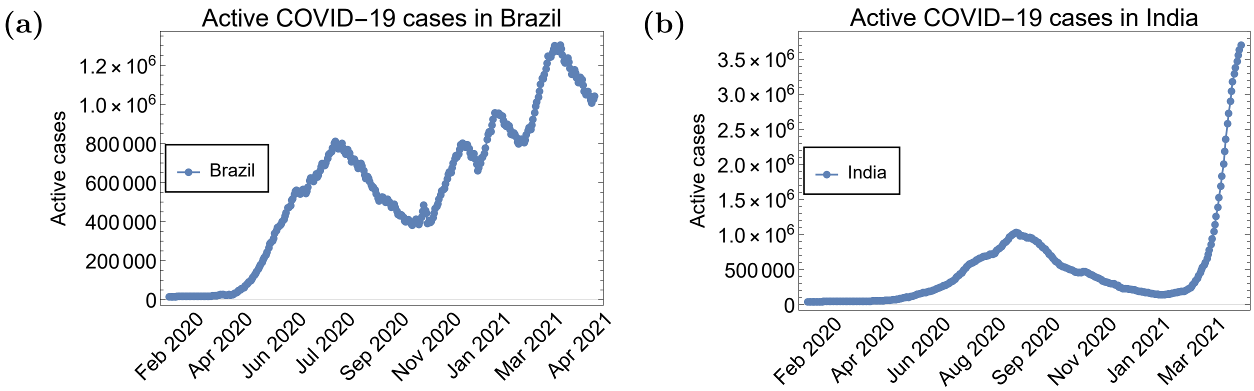

Figure 3: Active COVID-19 infection curves in a) Brazil, b) India, where more lenient policies were adopted. These countries are still struggling to contain the disease with a high number of active infections as of this writing. Data taken from [12]. US infections are shown in Figure 5.

are resistant to receiving vaccination. This justifies the need for better tools to assess the spread and quickly take action. Since the policy response varied by country, these tools should consider the local environment of the policies to investigate their effect in the dynamics.

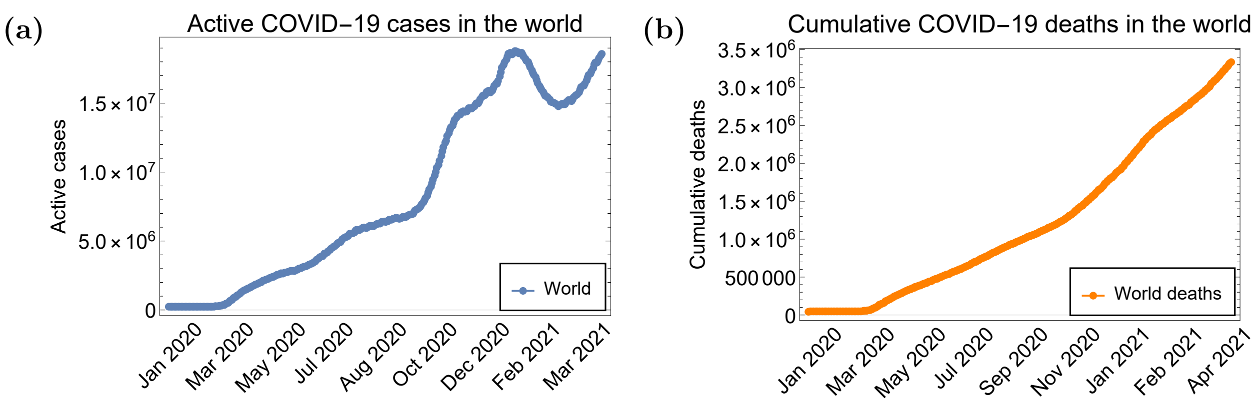

Figure 4: a) Worldwide active COVID-19 cases as a function of time. b)Worldwide cumulative COVID-19 deaths over time. The trends indicate that, in average, the world is still struggling to contain the pandemic as of this writing. Data taken from [12].

In the US, as of March 31st, 2021, the total number of infections still exceeded $31,000,000$ and the death toll was approximately $567,000$. The total infections curve and the total deaths over time are presented in Figure 5. The governmental response varied widely by state, which, probably, complicated the dynamics and the containment efforts. Active infections began dropping when vaccination became widely available, with first shots distributed around December 2020 for front-line healthcare workers and in January 2021 for other front-line workers and at-risk populations. It

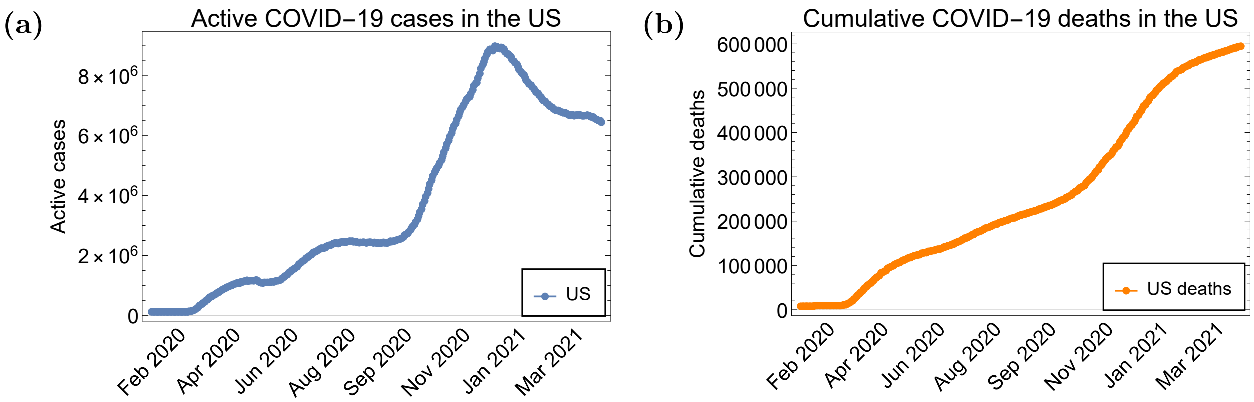

Figure 5: a) Number of COVID-19 active cases as a function of time in the US. b) Cumulative COVID-19 deaths over time in the US. The trends indicate that containment seems likely, probably due to widespread vaccination. Data taken from [12].

must be acknowledged that COVID-19 vaccines were developed in record time, with initial doses available in less than a year. In comparison, the previous record time was 4 years for the mumps vaccine, achieved in the 1960s. This faster development was achieved in part thanks to extensive research on associated viruses (e.g., SARS-COV, first detected in China at the end of February, 2003 [13]), and because of development of faster ways to manufacture vaccines [14]. For future pandemics, a vaccine may also be able to be promptly developed, but there is no guarantee [14]. This point is even more important as there is evidence that suggest humankind will likely have to face more pandemics in the near future [15], [16], and that novel, more resistant, virus and bacteria may be expected to appear [17].

By this point, it hopefully has become clear to the reader that forecasting the dynamics of an infectious disease is an extremely complicated task. There are several factors at play, including, but not limited to, awareness in the community, local and federal policies imposed to the population, behavioral changes in the population, the type and characteristics of virus, reinfections, availability of a vaccine, etc. To add a further layer of complexity, one must account for the compliance with the policies, stochasticity, and demographics of the population. Each one of these considerations add complexity to the model and increases the computational cost associated with forecasting. For example, a feasible way to account for demographics is to consider the role of "essential" workers (those who must interact with the public as part of an essential job). Gasoline, groceries, and medical care are examples of such essential businesses, and these "essential" workers are therefore more likely to interact with individuals than "non-essential" workers during a lockdown. For the purpose of this work, we refer to essential workers as those individuals who must keep interacting (face-to-face), with others during a pandemic due to the nature of their work and non-essential workers as those who can work from home and suffer from limited economic hardship due to a lockdown. It has been suggested that face-to-face workers are unfairly impacted by a pandemic [18], [19]. Essential workers often continue to work at essential locations out of economic necessity. Non-essential locations are public spaces and all other businesses that are able to conduct their usual operations remotely. As a result of the economic impact of a pandemic, non-essential workers may be laid off from their jobs, so they are at greater risk for eviction and may seek out existing essential jobs. Thus, pandemic lockdowns may exacerbate economic disparities and simultaneously put economically disadvantaged communities at greater risk of disparities in infection rates.

To better define the scope of this work, a brief discussion of the most common NPI policies implemented in the US is included below. We explain the definition of each policy, how it aims to reduce infections, and what possible population responses to these policies may exist. We also specify the first two policies in the context of this work, as we only assess their impact onto the dynamics of the infection in our model.

- **Lockdown policies:** A lockdown is a procedure that restricts the mobility of individuals to avoid an immediate risk affecting all or some part of a population. In the context of a pandemic, this policy is implemented to flatten the infection curve by reducing the number of encounters between healthy and infected individuals. It is usually implemented at the beginning of an outbreak to limit the number of infections in the population. However, not all individuals are able or willing to abide to this policy. Our social system of organization demands that some individuals keep working to provide essential services during a pandemic, e.g., grocery store workers who must interact with the public. Alternatively, others may willfully decide to ignore lockdowns and congregate without regard for the disease. For the purpose of this work, we consider only lockdown policies that restrict the interaction of non-essential workers at non-essential locations, without change to the time spent at essential locations.

- **Personal protection equipment (PPE) policies:** A PPE policy is the requirement to use personal protection equipment to reduce an immediate risk of infection. It is aimed at reducing the probability of infection during an interaction between susceptible and infected individuals, by means of a physical barrier that inhibits (partially or fully) the transmission of the disease. When the virus is airborne, effective PPE choices include masks and face-shields. As with lockdowns, not all people want or are able to abide to this policy. In this work we consider the effect of mask mandates and their compliance onto the dynamics of infection, assuming the policy requires all individuals to wear facemasks only at essential locations (defined above).

- **Social distancing policies:** Social distancing is the requirement to maintain at least 6 ft (2 m) of physical distance between any pair of individuals at all times. This policy is aimed to reduce the risk of contagion for diseases in which physical proximity increases the probability of transmission. While people are more willing to abide to social distancing than to lockdowns or mask policies, distancing is difficult to implement without a reduction in time spent in crowded spaces. We thus focus on lockdowns rather than distancing in our model.

- **Contact tracing:** Contact tracing is a set of strategies aimed to interrupt chains of transmission of the infectious disease. It involves keeping a registry of infected individuals' close contacts during the period in which they may have been infectious before being diagnosed with the disease. Health authorities, then, contact all close contacts and alert them so they can self-isolate and quarantine. This entire process may be conducted via phone calls or mobile apps with location sharing. The effectiveness of contact tracing relies in the stage at which it is applied, the quality of the data acquired, and the enforcement of quarantine/self-isolation requests. In the case of COVID-19, tracing had a small impact due to its rapid spread.

Mathematical models often struggle to capture all the of these features, or they become too complicated to be applicable to real situations. Any model must balance between complexity and applicability. That is, one must choose between having a model that captures even intricate details of the infection dynamics, and one that presents a coarse-grained approach but can be easily applied to real life situations. This can be greatly helped by endowing the model with features that have a physical meaning. This endowment simplifies the understanding, but it may be hard to achieve due to the interdependence of the parameters on the dynamics. Historically, mathematical models have been better as a retrospective analysis tool to fit real data and explain the dynamics of the spread. But a significant gain can be expected with a model that offers insights on policy effectiveness in a realistic scenario, and which is able to dissociate the roles of different groups into the outbreak.

Our proposed model is a modification of the SIR model that captures two fundamental features of the population: whether individuals are essential workers (those that must interact with the public, as defined above) or not and how risky their behavioral response to the outbreak is (whether they adopt or resist mask-wearing). In addition, we included features that are directly affected by lockdown or stay-home orders and mask usage: interaction time at essential locations and time spent at non-essential locations. At non-essential locations, we assume interactions are assortative: those that choose to wear masks avoid interacting with those who do not (referred as assortativity). Since policies are usually implemented locally in a community, our model gives insights on their effectiveness to contain the spread within the community. In Chapter 2, a qualitative analysis is conducted to infer the effect of a given policy into the dynamics of infections using different models. We describe simplified coarse-grained models for studying epidemic spreading in a community beginning with the classic SIR model and culminating in the LP-SIR model that accounts for assortativity, policies, and essential vs non-essential subpopulations. In Chapter 3, we apply this model to qualitatively describe the effectiveness of lockdowns and/or mask mandates given the community assortative structure described above. Some of the main findings are that mask mandates are not effective without lockdowns, lockdowns must be unrealistically perfect to work without mask mandates, and that essential workers may play a significant role in spreading and acting as a reservoir of the disease. We also show that the LP-SIR model can quantitatively recover the total infection dynamics of large populations with disparate lockdown policies (New York City, Texas, and California). We use this fitting to estimate the potential disparity between essential and non-essential workers and find that essential workers are at significantly greater risk of infection relative to non-essential workers for each region. This is particularly true for cautious essential workers (those that would wear a mask out of caution) as opposed to risky essential workers (those that only wear a mask if required by a policy). In Chapter 4, we study the implications of neighborhoods with diverse populations of essential workers, some of whom commute from one neighborhood to another. We find that an infection beginning in the neighborhood with fewer essential workers affects both communities equally, whereas an infection that begins in the neighborhood with more essential workers tends to have a significant impact on that community but a limited impact on the community with fewer essential workers. In Chapter 5, we summarize the work presented and discuss its implications.

2 Methods: Modelling of infectious diseases

There are several approaches to modelling infectious disease dynamics, including compartmental, stochastic, and network-based models, all of which can be tuned to add advanced characteristics as spatial structure, heterogeneity, age structure, among others. None can perfectly describe and predict the dynamics of an outbreak but instead can only be used to forecast or predict the effect of policies or societal decisions. There is always a trade-off between models, with some offering a simple qualitative description but overlooking many details, and others that can even achieve quantitative forecasts but are more complex and rely on large and accurate databases. In this section, some common types of models will be presented, including a brief description and their strengths and weaknesses.

2.1 Compartmental models

2.1.1 SIR model

A common approach for studying the spread of an infectious disease is to divide the population into compartments. The classical SIR model [20] divides the population into 3 compartments: Susceptible (S), Infected (I) and Recovered (R). This model describes the dynamics of the spread of the disease, which show an initial exponential increase in infections followed by a sudden decrease when the susceptible population starts to fade out. All individuals in a subgroup are assumed to behave identically, to have the same status, and to be subject to the same hazards. Another assumption is that recovered individuals cannot get sick again. These features are what is seen qualitatively in many real-world epidemics and are depicted in Figure 6, which also includes the interaction parameters for each compartment.

Mathematically, the SIR model is given by the following set of coupled differential equations:

$$\frac{dS}{dt} = -\gamma_{SIR}\frac{SI}{n}$$

$$\frac{dI}{dt} = \gamma_{SIR}\frac{SI}{n} - \delta I$$

$$\frac{dR}{dt} = \delta I$$

where n is the size of the population, S, I, and R represent the size at a given time of the susceptible, infected and recovered populations, δ is the recovery rate and γ_{SIR} is the infectivity rate in the SIR model. This system can be solved analytically under approximations, but it has no analytical solution for the explicit time dependence of compartmental sizes [21]. It is worth noticing that the size of each compartment changes with time according to $S(t)+E(t)+I(t)+R(t) = n$, so that the population, n, remains constant.

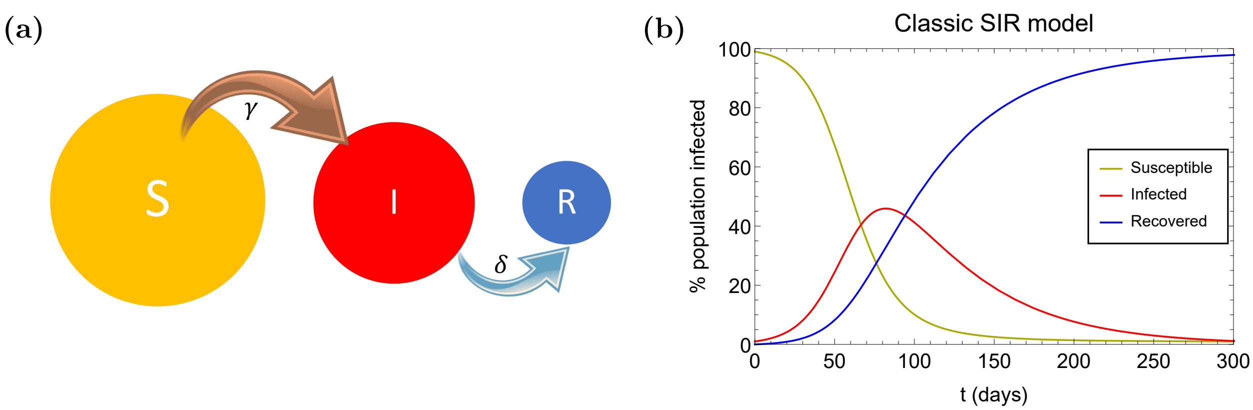

Figure 6: a) Compartments for the classic SIR model: Susceptible (S), Infected (I) and Recovered (R). The infection rate is γ_{SIR} and the recovery rate is δ. b) Example of the dynamics in a typical SIR model simulation with $R_0 > 1$, showing the initial exponential growth followed by a slow down to reach a peak, and a decrease whenever R_{eff} drops below 1.

To get a better intuition on the dynamics of the classic SIR model, it is useful to understand the physical processes described by each term. The factor $\frac{SI}{n}$ represents the number of interactions between the susceptible and infected compartments at a given time, normalized by the total population, which gives an estimate on how many susceptible individuals are at risk of contagion. If this factor is coupled with the infectivity rate, γ_{SIR}, the result is the number of new infections at a given time. The underlying assumption is that there is a continuous population, which is a reasonable approximation for large and well-mixed populations. The parameter δ can be recast as $\delta = \frac{1}{\tau}$, where τ is the average recovery time; that is, the time an individual takes since entering the infected compartment until fully recovering. As it was mentioned before, in the classic SIR model, there is no chance of a reinfection: all individuals leaving the infected compartment enter the recovered one.

A fundamental quantity, specific to a given disease, is the basic reproduction number, R_0, which is defined as the number of secondary infections arising from a single infected individual [22]. It is given by $R_0 = \frac{\gamma_{SIR}}{\delta}$. This number alone determines if an emergent infection will grow or die out: within the SIR model, if $R_0 < 1$, the infection will die out, whereas if $R_0 > 1$ it will grow. Notice that this number only gives the initial behavior of the infection, it does not give information on the dynamics at later stages.

In general, δ cannot be modified by behavioral policies, it solely depends on the specific disease and the provided healthcare. Instead, behavioral changes modify γ_{SIR}. Lockdowns and mask mandates produce a smaller effective infection rate due to either a reduction in the average amount of time that susceptible individuals interact with infectious individuals, or to a reduction in the infectivity per unit time of infectious individuals.

The basic reproduction number ignores the fact that the susceptible population is changing over time, which means that the number of new infections should be time dependent as well. To tackle this issue, an effective reproduction number can be defined: $R_{eff} = \frac{R_0 S(t)}{N} = \frac{\gamma S(t)}{\delta n}$. As it was previously mentioned, the infection first undergoes a phase of exponential growth, then slows down to reach a peak and finally decreases until it dies out. These stages in the dynamics correspond to different values for R_{eff}. If it is greater than 1, the infection grows, whereas if it drops below 1, the infection will gradually decrease until dying out (this phase is usually called "herd immunity"). At the peak of the infection curve $R_{eff} = 1$.

The greatest advantage of the classic SIR model relies in its simplicity and low computational demands. It helps to give a rough idea on how a particular disease would behave in a homogeneous, well-mixed population, which is large enough to be treated as a continuous variable. However, there are several limitations of this SIR model; the assumption of a homogeneous population, the lack of flexibility to accommodate for demographics, and the fact that there are diseases for which more compartments may be necessary. In reality, any community is composed of heterogeneous individuals, which complicates the dynamics. Additionally, there are infectious diseases that cannot be accounted for by the 3 considered compartments. For instance, to accurately describe HIV infection dynamics, it is necessary to add an asymptomatic compartment. For measles, there is an incubation period before individuals become infectious, so one must add an exposed compartment. For other diseases, such as influenza, reinfections need to be considered. There are more sophisticated variations of the SIR model that can account for diverse types of diseases, reinfections, demographics and even stochasticity, some of which will be considered next.

2.1.2 SIS model

For some infectious diseases, reinfections need to be considered as recovered individuals do not get long-lasting immunity, e.g. influenza and common colds. In this case, a model that considers only the susceptible and infected compartments is more appropriate. Infected individuals become susceptible again right after recovery. The equations for the model become:

$$\frac{dS}{dt} = -\gamma \frac{SI}{n} + \delta I$$

$$\frac{dI}{dt} = \gamma \frac{SI}{n} - \delta I$$

The physical intuition behind the model is similar to the one for the classic SIR. The term $\gamma SI/n$ gives the number of new infections at a given time, exactly as in the SIR model. The δI term still represents the fraction of the population which has recovered. In this case, it reenters the susceptible compartment instead of forming a separate one. The result is a model with two possible equilibria, $I = 0$ and $I = n(1 - 1/R_0)$, where $R_0 = \frac{\gamma S(0)}{\delta}$ is the basic reproduction number. As in the classic SIR model, if $R_0 < 1$ the infection never increases (i.e. $I = 0$ is the stable equilibrium), whereas if $R_0 > 1$, there is an outbreak and $I = n(1 - 1/R_0)$ is the stable equilibrium. Figure 7 shows the schematics for the SIS model alongside a simulation for the case $R_0 > 1$. Notice that the infection keeps going forever, as an equilibrium rate is reached, in which the same number of individuals are passing from S to I and backwards; that is, the rate of recovery matches the rate of infection.

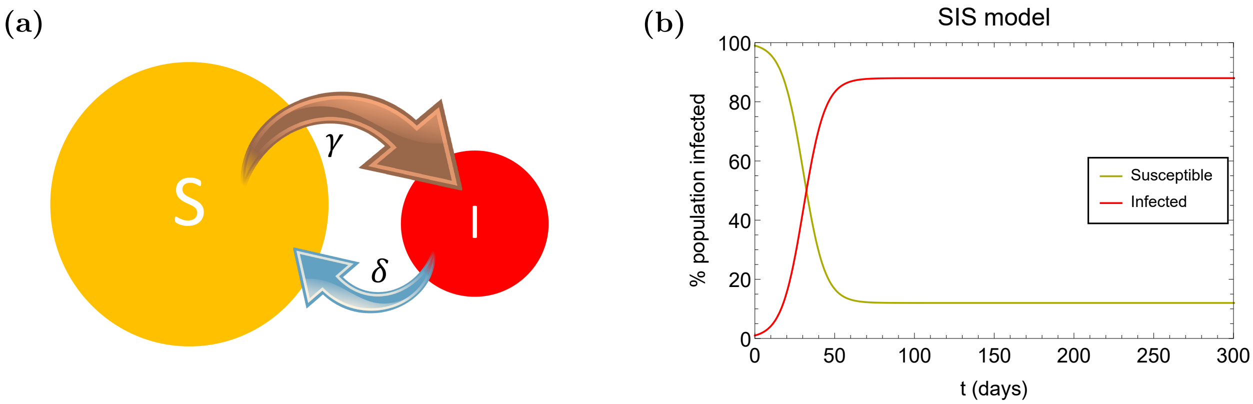

Figure 7: a): Compartments for the SIS model: Susceptible (S), and Infected (I); the infection rate is γ, and the recovery rate is δ. b) Simulation showing SIS model dynamics with $R_0 > 1$, where the equilibrium is $I = n(1 - 1/R_0)$.

2.1.3 SEIR model

The SEIR model accounts for diseases that have an incubation period by considering an additional category, the Exposed (E) compartment. The differential equations describing the dynamics for this model become:

$$\frac{dS}{dt} = -\gamma\frac{SI}{n}$$

$$\frac{dE}{dt} = \gamma\frac{SI}{n} - \sigma E$$

$$\frac{dI}{dt} = \sigma E - \delta I$$

$$\frac{dR}{dt} = \delta I$$

where $1/\sigma$ is the average length of the incubation period and all other parameters are the same than for the SIR model. In this framework, a susceptible individual becomes part of the exposed group after having contact with any infected person; afterwards, the exposed individual transitions to the infected group after the incubation period ends, when he becomes infectious. Notice that any susceptible must pass through the exposed compartment to become infected and infectious. Thus, the dynamics are similar to the SIR model but with a delayed peak, which depends on the incubation time $1/\sigma$. Figure 8 shows a schematic design of the interactions between compartments and depicts the dynamics of the SEIR model, which follows the same rise, slow down and fade out pattern described for the classical SIR model but with the delayed peak due to the incubation period of the disease.

(a) **(b)**

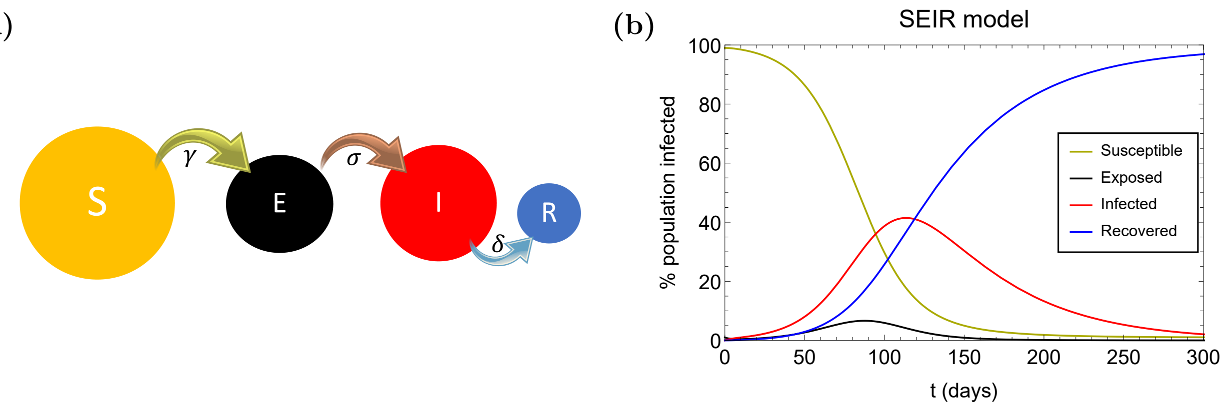

Figure 8: a) Compartments for the SEIR model: Susceptible (S), Exposed (E), Infected (I), and Recovered (R). The infection rate is γ, the incubation period is $1/\sigma$, and the recovery rate is δ. b) Simulation showing the typical SEIR model dynamics with $R_0 > 1$, showing similar behavior to the SIR model but with a delayed peak due to the incubation period.

In the context of COVID-19, the SEIR model allows to account for the incubation period of the COVID disease, which is estimated to be between 2-5 days after exposure [23]. By modifying the SIR model to including the Exposed compartment, the predictions are expected to better resemble real data by increasing the complexity, which also increases the computational cost. To achieve even more resemblance to real data, it is possible to account for the effect of asymptomatic individuals in the dynamics by introducing further compartments into the model, resulting in the so called SEAIR model (where A stands for asymptomatic). However, for the level of approximation considered in this work, modifying the SIR model suffices. The purpose was to understand the role of essential and non-essential workers in the spread of the disease rather than make quantitative forecast.

2.2 Stochastic compartmental models

One of the limitations of the conventional compartmental models is that they overlook noise effects and fluctuations that become important when reconciling the model to real world data. Modifications can be introduced to simplistic compartmental models to account for statistical fluctuations in several forms. The most common types are discrete Markov chain models, continuous Markov chain models and stochastic differential equations models [21]. A Markov process is one in which the state at time $t' = t + \Delta t$ depends only in the state at time t. In the case of this models, the states in question are $I(t')$ and $I(t)$, whose relationship is defined in a probabilistic manner. One of the biggest differences with deterministic compartmental models is their asymptotic behavior. In stochastic models a solution converges to a disease-free state even if the basic reproduction number of the infection is greater than 1 (i.e., $R_0 > 1$). Recall that in deterministic models, if $R_0 > 1$, an outbreak begins and there are solutions with a non-zero equilibrium state. Another difference is the smoothness of the solutions: deterministic models are of course smooth and well behaved, whereas, as the name hints, stochastic processes have random fluctuations that reflect the statistical nature of the parameters that determine the infection.

2.3 Local Policy-SIR model

While the SIR model qualitatively captures some of the dynamics of an infectious disease spreading throughout a community, a number of key features of real-world communities are not accounted for. Specifically, the SIR model assumes that all individuals are identical and indistinguishable, whereas real world communities are composed of heterogeneous individuals. The SIR model also assumes that all interactions have the same likelihood of infection occurring, whereas in reality the likelihood of infection will be reduced if the infected individual is wearing a mask. Thus, it is essential to add these features to the model in order to understand the costs and benefits of public policies involving non-pharmaceutical interventions (NPIs), such as total or partial lockdowns, quarantine, isolation, social distancing, mask mandates, and travel restrictions. Moreover, in the US, policies are highly heterogeneous, generally put in place by states or local governments, with only a few NPI policies enforced nationwide. This must be accounted for as well into the model.

In this section, we introduce a modification of the classic SIR model that accounts for local policies in a community and its diverse behavioral characteristics, the Local Policy-SIR (LP-SIR) model. Accordingly, the compartments from the classic SIR model are subdivided according to the behavior of individuals towards mask usage and the essentialness of their jobs. In this work, an individual is defined as "essential" worker if he/she must keep interacting face-to-face with others during a pandemic. "Non-essential" workers are defined as the individuals who can easily transition to working remotely from their homes. This is distinct from the legal definition of essential and non-essential workers, where some workers (e.g., lawyers) may be legally essential but work from home. The model also provides two kinds of locations at which interactions can happen: essential locations (meaning business that cannot operate without face-to-face workers) and non-essential locations (meaning businesses that can permit remote work). Essential locations are the workplaces of essential workers (as defined above) where they keep interacting face-to-face with other individuals. Non-essential locations are all the other businesses and public spaces where interactions and infections may happen. This distinction enhances the model and allow a better understanding of the dynamics of an infectious disease in a local community.

In the social model considered in this work, essential businesses are constrained to remain open to the public during a pandemic regardless of the severity of the infection. Societal needs such as energy, food, transportation, and healthcare cannot be adequately satisfied without some economic sectors remaining open. Essential employees have thus to keep working regardless of the circumstances. The requirement that a fraction of the population cannot reduce their interaction with infected individuals may have important impacts on the dynamics of the disease. Essential employees may represent a potential source for the epidemic to continue to spread (as they are forced to interact with the potentially infected public) and are potentially at greater risk to contract the disease for the same reason. Due to the nature of their work, essential employees interact on average with more people and for longer periods than non-essential workers. For instance, a grocery store employee is compelled to interact with more individuals during his shift than an employee who only does online meetings. Restaurant and bar workers represent a unique potential for exposure, as while those businesses are open the customers cannot wear a mask while consuming the food or drink served by the business. Accordingly, in the LP-SIR model, the population is divided into compartments based on the type of job they have, their attitude towards mask usage, and their infection status. Two types of jobs are considered: essential (E) and non-essential(N). Workers are also divided in cautious (c) and risky (r) groups, depending on whether they are willing to wear masks or not in non-essential public locations. In addition, the main compartments of the SIR model: susceptible (S), infected (I), or recovered (R) are considered for the status regarding the disease. Each main compartment is labeled using two subscripts: one for their type of job and the other for their attitude towards mask usage. In total, there are 4 different subscripts ($_{Ec}$, $_{Er}$, $_{Nc}$, $_{Nr}$) for each of the main compartments, giving a total of 12 groups within the population (S_{wm}, I_{wm}, and R_{wm} with $w = E, N$ and $m = c, r$).

In the LP-SIR model, the spatial structure is given in the form of two kinds of locations at which interactions happen: non-essential and essential locations. At non-essential locations, where people can be selective, we introduced assortativity to reflect the tendency of people to interact preferably with individuals sharing similar characteristics. At essential locations, interactions take place between all groups in the population since everyone needs to visit essential locations to satisfy basic needs. These features are a key component to reproduce real dynamics because NPI policy decisions are generally applied to locations. Lockdowns can prevent anyone from entering a specific store but generally cannot prevent people from interacting with one another on the street, whereas a mask mandate can be set up at essential businesses, but they are generally not enforced outside them or in open areas. Non-essential locations include public areas and workplaces consisting mainly of non-essential employees (i.e. public and private companies which can arrange work from home for their employees), whereas essential locations refer to workplaces that encompass a majority of essential workers (e.g. grocery stores, hospitals, pharmacies, utility related facilities, etc.).

Due to the differences in interactions of individuals at essential vs non-essential locations, the infectivity of the disease (γ) will depend on the context of both the people interacting, as well as the governmental policy that governs mask usage (which may be location dependent). Thus, the model provides infectivity rates that reproduce these conditions. At non-essential locations, there is no mask policy, so the infectivity depends on the intrinsic risk of each individual at contact: γ_r (γ_c) is the infectivity for a contact between an infected risky (cautious) individual and a susceptible risky (cautious) one. These two parameters are determined based on the inward and onward protection facemasks offer against transmission. At essential locations, the mask policy decreases the risk of contacts involving risky individuals according to the function $\gamma_r^{(p)} = \gamma_r - \mu(\gamma_r - \gamma_c)$, where μ is the percentage of individuals complying with the mask policy. Figure 9 summarizes the possible interactions at each type of location including the associated infectivity. At each contact one person is susceptible and the other is infected, the arrow indicates the direction of the transmission.

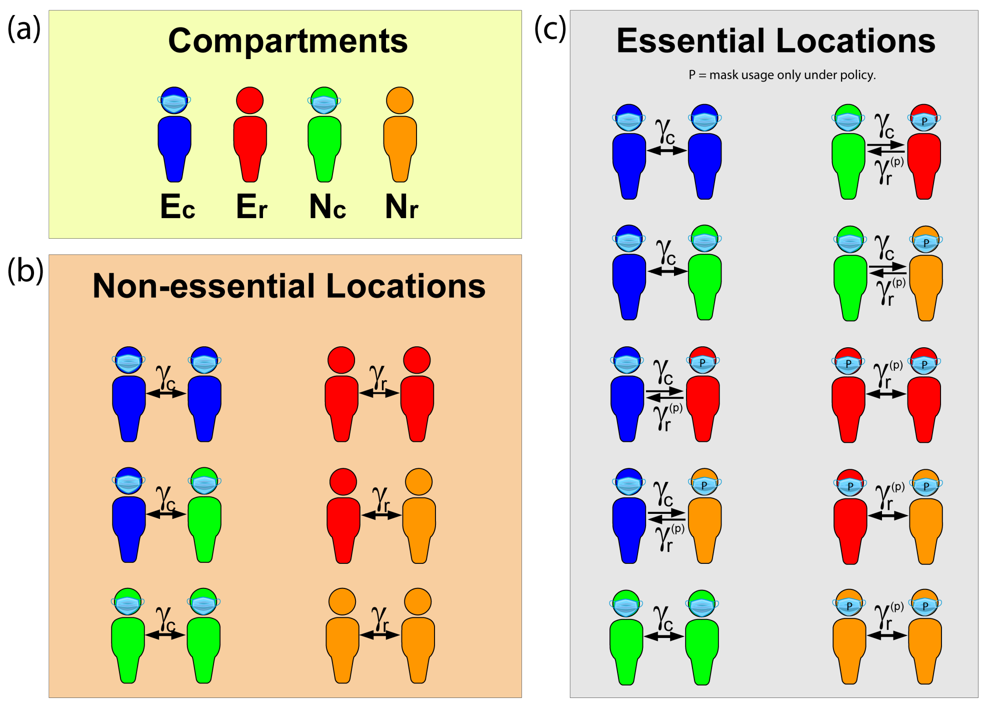

Figure 9: a) Compartments for the LP-SIR model: Essential cautious (E_c), Essential risky (E_r), Non-essential cautious (N_c) and Non-essential risky (N_r). b) Possible interactions at non-essential locations. Due to assortativity risky (cautious) people interact only with other risky (cautious) individuals. There is assortativity but no mask mandate, so the infectivity for contacts between risky individuals is larger than the one for contacts between cautious (i.e. $\gamma_r > \gamma_c$). c) Possible interactions at essential locations. There are more possible interactions since there is no assortativity. Infectivity involving risky individuals is reduced according to the mask mandate compliance. Arrow indicates direction of transmission.

The model also features time-interaction parameters that control the strength of interaction as a fraction of time (in a day) spent at a particular kind of location by a certain type of workers. They are labeled by the type of location (α= non-essential locations, β=essential locations) and have a sub-index for the type of workers they refer to ($_E$=essential workers, $_N$=non-essential workers). There are four time-dependent parameters: α_E, α_N, β_E, and β_N. Essential workers spend time proportional to β_E at their workplaces and proportional to α_E at public locations that are not associated with their workplace (e.g. a bar or a public park). Non-essential workers spend time proportional to β_N at essential workplaces (e.g. the time spent grocery shopping) and time proportional to α_N at their own workplaces or in other non-essential locations (bars or public parks).

The structure of the LP-SIR model naturally allows to implement two NPIs: lockdowns (meaning business closures) and facemask mandates. α_N and α_E are affected by lockdowns, whereas β_N and β_E are only affected by reduced operations. Likewise, mask mandates are modeled to decrease the infectivity at essential locations (depending on the compliance, μ). We used the LP-SIR model to understand the effect of different NPIs on the overall dynamics of the population, as well as to forecast the differing effects these policies have on specific subgroups.

Intuitively, all these assumptions should reflect the location-associated dynamics of the spread. Essential workers are expected to have a considerable influence spreading the infection because they must still show up at their usual essential workplace [24]. Meanwhile, risky individuals should also have a strong impact as the preference to not wear a mask carries an increased risk of contagion. Within this context, we showed that indeed, the LP-SIR model predicts that essential workers are at a higher risk of infection due to their workplace requirements, and that risky people are the main drivers of the spread when no lockdowns on non-essential workers are imposed, even under mask usage.

In summary, the structure of this model allows to consider the impact of initial conditions, compartmental sizes, compliance with mask mandates, interactions at essential and non-essential locations and assortativity between compartments on the infection dynamics. Assortativity is included by neglecting interactions between risky and cautious individuals at non-essential places. This is a significant approximation of the likelihood of interaction between cautious and risky individuals, but greatly simplifies the model. Two local policies are accounted for by adjusting the location-dependent parameters: lockdowns at non-essential places and mask mandates at essential locations. Lockdown policies are modeled by reducing α_N and α_E, the time-interaction at non-essential locations. In particular, a total lockdown of non-essential workers can be analyzed by choosing $\alpha_N = 0$. Likewise, the effect of a reduced shift policy for essential businesses can be analyzed by reducing β_E. At essential locations, mask policies reduce the infectivity of contacts including an infected risky individual, from γ_r to $\gamma_r^{(p)} = \gamma_r - \mu(\gamma_r - \gamma_c)$, where μ is the degree of compliance with the mask policy.

Mathematically, the LP-SIR model corresponds to a set of coupled partial differential equations that can be solved numerically. The equation for the rate of change of the susceptible population is:

$$\dot{S}_{wm} = -S_{wm}\left[\alpha_w\gamma_m(\alpha_E I_{Em} + \alpha_N I_{Nm}) + \beta_w\beta_E(\gamma_c I_{Ec} + \gamma_r^{(p)} I_{Er}) + \beta_w\beta_N(\gamma_c I_{Nc} + \gamma_r^{(p)} I_{Nr})\right] \quad (1)$$

where w ($w = E, N$) labels the type of worker, with E indicating essential workers and N non-essential workers, respectively), and m ($m = c, r$) designates behavior towards mask usage, with c indicating cautious individuals who prefer to wear masks regardless of the local policies, and r indicating risky individuals who prefer to wear masks unless required by local policy. Each term in equation (1) can be physically interpreted as defining the interaction between two distinct groups at a particular location for the typical duration of their interaction. For example, the term $S_{Ec}(t)\alpha_E\gamma_r\alpha_E I_{Er}(t)$ considers interactions between susceptible cautious essential workers and infected risky essential workers at non-essential locations with an infectivity γ_r (as the risky person would not wear a mask at non-essential locations). Each term in equation 1 is isomorphic to an SIR equation, which is easily seen by taking $\gamma_{SIR} = \alpha_E\gamma_r\alpha_E$, but the dynamics are complicated by the interplay between terms. The equations for the infected and recovered populations are similar to the conventional SIR model:

$$\dot{I}_{wm}(t) = -\dot{S}_{wm}(t) - \delta I_{wm}(t) \tag{2}$$

$$\dot{R}_{wm}(t) = \delta I_{wm}(t) \tag{3}$$

which means that the dynamics for the transition from the infected compartment to the recovered one will be SIR-like.

In following sections, we studied the dynamics of the model by varying the location dependent parameters. We considered different policies by carefully selecting values for the time interaction parameters, and we show how they change the overall dynamics of an outbreak.

3 Results

In this chapter, the results of a series of simulations are presented, starting with the classic SIR model, and adding complexity layers until developing the full LP-SIR model. The values for the infectivity rate, recovery rate, and mask compliance were taken from data in the literature, as explicitly indicated in each part. Normalization is carried over each compartment to avoid size-related effects in the analysis unless explicitly noted.

3.1 Classic SIR model

For a classic SIR model, the infectivity is $\gamma_{SIR} = \alpha^2 \gamma_{eff}$, with α the average fraction of time spent by individuals interacting with others in a day. In this section, we assume a regular workday with no lockdown protocols, with $\alpha = 8/24$, which models the spread dynamics without any governmental intervention. The value for γ_{SIR} has been estimated previously in [25] finding $\gamma_{SIR} \approx 0.456$ at the beginning of the infection, which results in $\gamma_{eff} = 4.104$. Other works find values in the same ballpark as γ_{SIR} [26], [27]. The recovery rate was taken as $\delta = 1/14$ $1/days$ since the average recovery time has been estimated as 14 days; according to the CDC [23], 95% of infected individuals can no longer produce replication-competent virus after 15 days. Figure 10a shows the results for all compartments for $\gamma_{SIR} = 0.456$, and $I_0 = 1 \times 10^{-6}$ in a population normalized to 1. The resulting infection curve follows the dynamics of the classic SIR model with an exponential increase at first, a slowdown to reach a peak, and a fading out region until the infection dies out. Notice that the infection curve indicates that all population would be eventually infected, with more than half of the population infected with COVID-19 at the peak. This follows from the assumption that no policy is implemented by the government nor there are behavioral changes in the population, which are both unrealistic assumptions. In a real situation, the infectivity and/or recovery rates change due to several factors including, but not limited to, implemented policies, provided healthcare, behavioral changes, among others. Nevertheless, the bare SIR model is still useful as it gives an estimate on how the outbreak may look in the absence of interventions, which is very important at early stages of the outbreak where this assumption holds and quick policy decisions are needed. In Figure 10b, we simulate the effect of a partial lockdown in the population by reducing α to $5/24$. The peak value of the infection curve decreases significantly, and it is delayed, which is expected, since this choice corresponds to simply reducing the infectivity. As we mentioned before, a lockdown results in a reduction of the infectivity as the number of contacts that might result in infections are lowered.

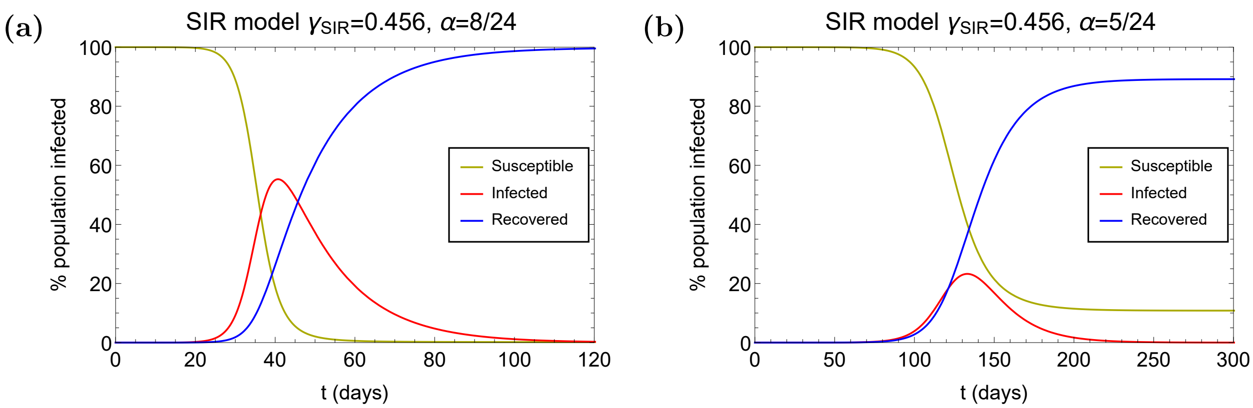

Figure 10: Results for the classic SIR model with infectivity rate $\gamma_{SIR} = 0.456$ and recovery rate $\delta = 14\ 1/days$ assuming: a) No interventions from the governments nor behavioral changes in the population ($\alpha = 8/24$), b) A partial lockdown of the population ($\alpha = 5/24$). Note that the infections are both significantly reduced, and the peak infections are delayed by many months.

It is important to remark that, using the classic SIR model, the effect of NPIs is averaged over all population, failing to capture important details that arise from heterogeneities between the groups. For instance, simulating a lockdown with this simple model would be misleading because, in reality, not all individuals would be capable of (or willing to) reducing their interacting time to the same degree, and interactions between all members of the population are assumed to occur at the same location. Similarly, a mask mandate corresponds to a reduction in the infectivity, but it would again be an averaged effect as it overlooks effects of masks incorrectly worn, and that of individuals not willing to wear them unless required by law.

3.2 SIR model with behavioral characteristics and spatial structure

From the previous results, it is clear that the assumptions in the classic SIR model are too coarse to meaningfully describe the dynamics of transmission in a heterogeneous population. Several ways of addressing this issue have been explored: considering different age groups [28], [29], adding an incubation period [30], [31], adding exposed and asymptomatic individuals [32], [33]. In this section, a more limited LP-SIR model was considered, where only spatial structure and mask usage characteristics are considered. As far as we know, the distinction between cautious and risky individuals has not been implemented before. By adding this layer of complexity to the classic SIR model, heterogeneous characteristics are allowed onto the dynamics, and this serves as a mid-step to building the full LP-SIR model. The advantage of this step-by-step building is that the effects of new groups onto the dynamics can be better traced. In this section, spatial structure was implemented into the model by providing two types of locations for people to interact: essential locations and non-essential locations. Behavioral characteristics (m) were also added by considering cautious (c) and risky (r) individuals. Thus, each of the main SIR compartments is divided in two, resulting in a total of 6 groups: S_c, S_r, I_c, I_r, R_c, and R_r, where S_c is the population of cautious individuals that are susceptible to the disease, S_r is the population of risky individuals that are susceptible to the disease, I_c is the population of cautious that are infected with the disease, I_r is the population of risky that are infected with the disease, R_c is the population of cautious that recovered of the disease, and R_r is the population of risky that recovered of the disease. These assumptions result in dynamics that differ depending to the location, where the key factor is relaxing the homogeneity of the population. The equations for the susceptible groups ($m = c, r$) in this model are:

$$\dot{S}_m = -S_m \left[\alpha^2 \gamma_m I_m + \beta^2 (\gamma_c I_c + \gamma_r^{(p)} I_r) \right] \tag{4}$$

The dynamics were numerically integrated with the population evenly divided between the cautious and risky groups to avoid size effects into the resulting dynamics. As we discussed before, in the classic SIR model, $\gamma_{SIR} = 4.104$ is the average infectivity of a contact between two individuals in the population. In this modified model, this value is the result of a weighted average of the infectivities of cautious and risky populations. By considering that they interact at essential and non-essential locations for the same amount of time, it is possible to determine the value of γ_r. To calculate γ_c, the protection provided by facemasks was considered. Previous research suggests that using facemasks reduces the transmission probability to 0-30% [34]. In this work, we considered that masks reduce the probability of transmission to 20% (i.e., they are 80% effective). In [24], it is pointed out that masks provide more outward than inward protection. This feature is accounted for by $\gamma_r^{(p)}$, the infectivity under a mask policy at essential locations, and μ, the compliance with the mask policy. So, the infectivity for contacts between an infected risky individual and any other susceptible is taken as $\gamma_r^{(p)} = \gamma_r - \mu(\gamma_r - \gamma_c)$ whereas the infectivity for contacts between infected cautious individuals and any other susceptible is taken as γ_c. At non-essential locations, the infectivity of a contact between risky individuals is $\gamma_r = 15.68$, and the infectivity for contacts between cautious individuals is $\gamma_c = 0.04\gamma_r = 0.627$ due to the mask usage, which drastically reduces it. Notice that the compliance is embedded into the model through the parameter μ, which was set as 85%. The initial conditions were set to $I_0 = 1 \times 10^{-4}$ for both groups, and the recovery rate was $\delta = 1/14\ 1/days$, as in the previous section.

Due to the spatial structure, there are two locations for interactions between cautious and risky individuals. As a first approach, we considered scenarios where interactions happen only in one of the locations. In the first scenario, all interactions happen at non-essential locations, where assortativity is present, so a flattened infection curve for the cautious compartment is expected. In the second scenario, where individuals interact only at essential locations, all compartments should be impacted equally as a result of the mask policy. Indeed, Figure 11a shows the results for the first scenario, with $\alpha = 8/24$. There are striking qualitative differences between the infection curves for risky and cautious individuals interacting only at non-essential locations. The peak for the cautious compartment not only occurs later but it also almost vanishes; that is, being cautious "flattens the curve". The cautious population sees a greater benefit because of mask usage. In the second scenario, we find that both the cautious and risky populations have the same infection curve due to the mask mandate. Thus, the mask requirement ensures that all compartments are exposed to equivalent hazards as depicted in Figure 11b, where $\beta = 8/24$. Paradoxically, the equivalent hazard comes at the expense of the cautious population, they see their hazard increase when they visit essential locations (where there is no assortativity) and are forced to interact with the risky population. As this model does not consider assortativity for essential locations, if the mask policy is not enforced, the risk skyrockets, because of interactions between risky and cautious at a higher risk, coming from the assumption that masks provide no inward protection. As for interactions at essential locations, there is a homogeneous mixing coming from mask enforcement. If a large fraction of individuals does not wear masks, the contacts leading to infections become extremely high, which indicates the importance of complying to the mask policy.

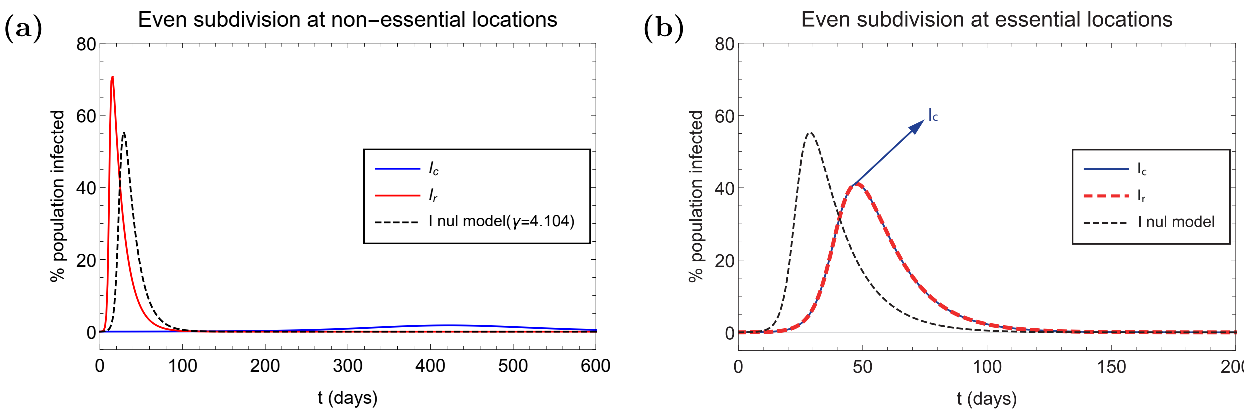

Figure 11: Results after adding the cautious/risky and the essential/non-essential locations distinction along with assortativity at non-essential locations. a) Interactions at non-essential locations show the infection curve for cautious occurs later and is almost vanishing; clearly, being cautious “flattens the curve”. b) Interactions at essential locations shows both risky and cautious individuals are exposed to the same hazards. “Null” model refers to a simple SIR model (without cautious/risky subdivisions) with an infectivity $\gamma_{SIR} = 4.104$.

Both scenarios described above can be understood in terms of utopian policies. The first scenario is equivalent to a policy closing all essential locations and letting people move freely at non-essential places, where people self-organize and interact with alike individuals only. Cautious individuals are almost unaffected and risky ones are penalized with a high outbreak. The second scenario corresponds to closing all non-essential locations but allowing all people to interact at essential ones under a mask policy for everyone, which results in a homogeneous mixing. In real life, not all people interact at essential businesses for the same amount of time. To illustrate this point, consider the case of essential workers at a grocery store. Employees usually complete at least an 8 h shift per day whereas shoppers spend at most a couple of hours at the store. This potentially increases the risk of essential workers for infection in an inequitable manner, since essential workers spend more time interacting with the population than a non-essential worker does.

Since the sizes for cautious and risky compartments may not be equal, numerical integration of equations 2-4 with different percentages of cautious compartments was considered to analyze the size effects onto the dynamics. Figure 12a-d, show the results when the fraction of risky population is 25% and 10% respectively. At non-essential locations (Figures 12a,c), we found that sequentially decreasing the risky fraction decreases the peak for risky people but increases it for cautious. This is due to the increase in the fraction of population for cautious people, which increases S_c and results in the increased and earlier peak. Conversely, at essential locations (Figure 12b,d), the peaks monotonically decrease if the fraction of risky individuals is reduced. This is expected since, at essential locations, there is no assortativity, so all individuals interact in the same manner giving a homogeneous mixing with a reduced infectivity (that depends on compliance to the mask mandate).

The LP-SIR model also allows to combine interactions at both essential and non-essential locations, which better resembles a real situation. In this section, both cautious and risky individuals were restricted to spend the same amount of time at each location. If this restriction is removed, the expected dynamics would be a weighted average of the dynamics at each individual location (weighted by the time spent at each kind of location), which does not offer new insights and is therefore omitted.

The complexity of accurately modelling infectious disease dynamics should be clear given the qualitative differences in the models considered in this section. By adding essential/non-essential locations and cautious/risky distinctions, we gained a better understanding of the hazard ratio between subpopulations and its dependence on the location of interactions, but analysis became more cumbersome. A physically relevant meaning of the parameters of the model can help to better

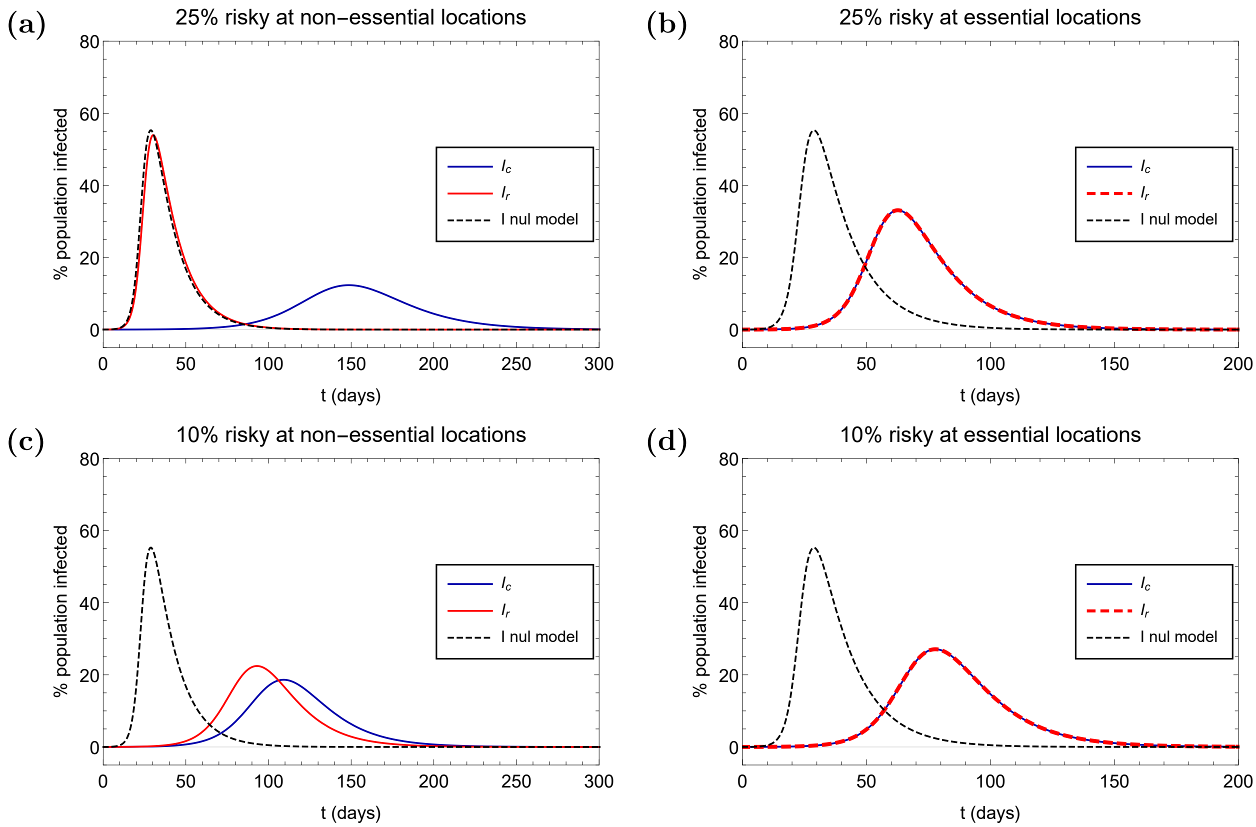

Figure 12: SIR-like model with behavioral characteristics and spatial structure. Dynamics for different ratios of risky/cautious individuals by the type of location at which interactions take place. a) 25% risky individuals and 75% cautious individuals interacting at non-essential locations. Both groups do not mix due to assortativity. b)25% risky individuals and 75% cautious individuals interacting at essential locations. Both groups mix homogeneously due to the mask policy. c) Same as in a) for 10% risky & 90% cautious. d) Same as in b) for 10% risky & 90% cautious.

interpret the resulting infection dynamics and to have a better intuition on the dynamics of spread of the infectious disease, particularly in the context of a heterogeneous population.

3.3 LP-SIR model: Adding Job Types

In the framework we considered here, essential businesses are constrained to function during a pandemic at nearly normal hours. Otherwise, needs such as energy, food, transportation, and healthcare could not be adequately satisfied. Essential employees must therefore keep working regardless of the circumstances, so their role in the spread of the disease cannot be overlooked. The population was subdivided into essential workers and non-essential workers, where each may spend different times at a particular kind of location. This provides a more realistic model, accounting for the asymmetry between essential workers that need to attend their usual workplace, as well as non-essential workers that can easily work from home. As a reminder, there are 4 subgroups for each of the SIR compartments: E_r, E_c, N_r, and N_c, which correspond to essential risky workers, essential cautious workers, non-essential risky workers and non-essential cautious workers, respectively.

We first considered an LP-SIR model with even subdivisions for both cautious/risky and essential/non-essential workers. In this first stage, the interactions had the same restriction as in the previous section: essential (non-essential) workers are permitted to interact at essential (non-essential) locations only. They all work their normal shifts of 8 h per day, so: $\alpha_N = 8/24$, $\alpha_E = 0$, $\beta_N = 0$, and $\beta_E = 8/24$. This corresponds to the case of essential worker population working at their jobs for 8 h/day, the non-essential worker population working at their jobs 8 h/day, but essential and non-essential workers never interacting. As in the previous section, the infectivity was chosen as $\gamma_r = 15.68$ for contacts between risky individuals at non-essential locations, $\gamma_c = 0.627$ for contacts between cautious individuals at non-essential locations (lower due to mask usage), and $\gamma_r^{(p)} = \gamma_r - \mu(\gamma_r - \gamma_c)$ for contacts involving a risky individual at essential locations, with $\mu = 0.85$. The recovery rate was set to $1/14$ $1/days$, and the initial infections $I_0 = 1 \times 10^{-6}$ for each compartment. Figure 13 shows that an infection appears only for non-essential risky (N_r) individuals. Notice that this is consistent with the situation in which people interact only at non-essential locations presented in the previous section, and thus, the infection does not spread to essential workers (see for example Figure 11a). This latter result was traced back to a high mask compliance of $\mu = 0.85$. If μ is decreased below 80%, then infections happen for all but the N_c compartment as shown in Figure 14 for the particular case $\mu = 0.65$. This means that mask usage, in fact, flattens the curve. It also emphasizes the importance of complying with the mask policy.

A key observation from results in Figure 14 is that the infection for the N_r compartment has fast dynamics whereas both the E_c and the E_r groups have slower dynamics (also, E_c and E_r have the same infection curve, as expected, from them interacting only at essential locations). As in the previous section, this arises due to the mask policy and the restriction in the locations for

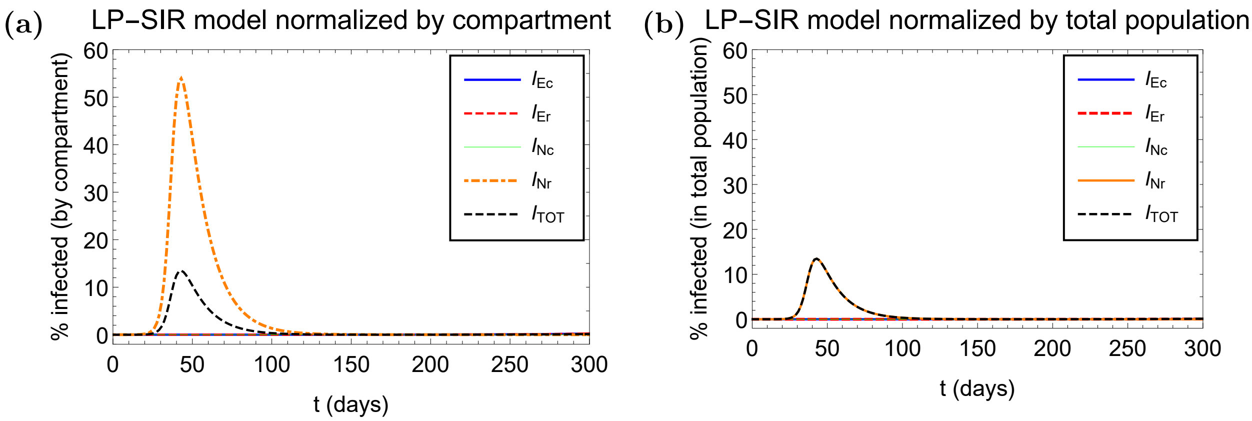

Figure 13: LP-SIR model with even subdivisions of compartments with compliance $\mu = 0.85$, normalized by a) each compartment and b) the total population. $\alpha_N = 8/24$, $\alpha_E = 0$, $\beta_N = 0$ and $\beta_E = 8/24$ indicating essential (non-essential) workers interact only at essential (non-essential) locations. Due to the mask policy, only the N_r compartment shows an outbreak (the N_c group does not due to properly wearing a mask), which leads to no outbreak at essential locations.

interactions. Facemasks reduce the risk at essential locations, whereas restricting cross interactions between essential and non-essential workers reduces the number of contacts that potentially lead to infections. By looking at the total infection curve in Figure 14b, it is clear that this model is able to explain the presence of two peaks in the curve by means of the differing types of dynamics. This is a feature observed in real infection curves for COVID-19 in many states within the US.

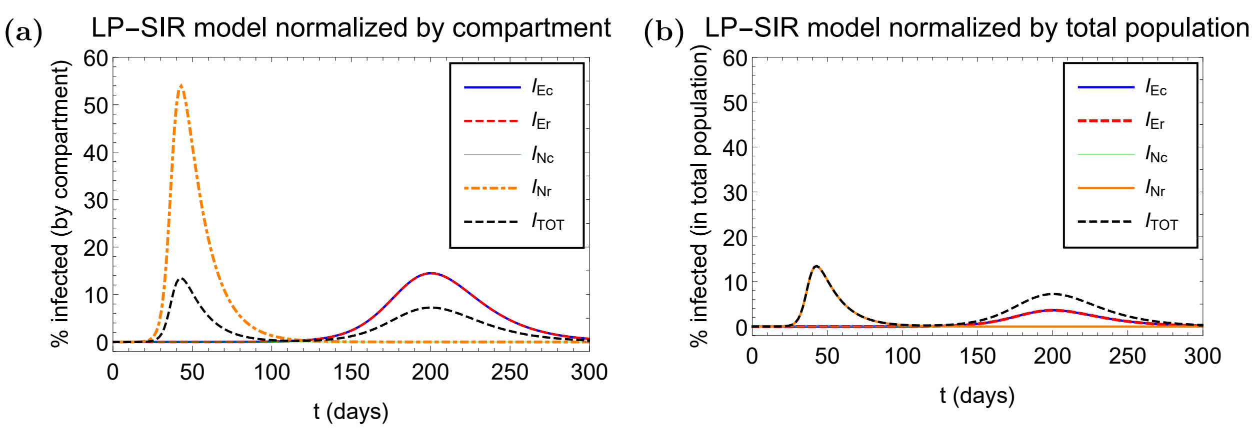

Figure 14: LP-SIR model with even subdivisions of compartments with $\mu = 0.65$. $\alpha_N = 8/24$, $\alpha_E = 0$, $\beta_N = 0$ and $\beta_E = 8/24$ indicating essential (non-essential) workers interact only at essential (non-essential) locations. If $\mu < 0.80$, all but the N_c group have infections, indicating the importance of mask policy compliance. Essential compartments show equal dynamics, as expected. The N_c compartment does not show an outbreak as a result of assortativity at non-essential locations.

We performed a second calculation, intended to relax the previous restrictions on where interactions happen. In this analysis, the parameters were chosen as: $\alpha_N = 8/24$, $\alpha_E = 1/24$, $\beta_N = 1/24$, and $\beta_E = 8/24$, which represents a situation in which non-essential workers spend 1 h at essential locations and essential workers spend 1 h at non-essential locations while doing their regular 8 h shift at their corresponding jobs. The resulting dynamics, plotted in Figure 15, show that each of the compartments have different infection curves and do not display the purely bimodal peaks found in Figure 14. Risky workers are more affected than cautious (consistent with findings in the previous section). Since $\alpha_N \gg \beta_N$, the infection curve for non-essential workers closely resembles the case in which interactions happen only at non-essential locations. There is, an averaging effect between N_c and N_r due to the 1 h they spend at essential locations, which increases the infection for the N_c group. Conversely, the infection curves for essential workers look closer together than non-essential workers. This is consistent with the expectation of equal curves for interactions at essential locations, which is due to the mask policy averaging the infectivity. The higher peak for E_r is a result of setting $\alpha_E = 1/24 \neq 0$ (i.e. essential workers interacting at non-essential locations for 1 h), which breaks the symmetry between E_c and E_r, and gives a higher peak to risky individuals because they do not wear masks.

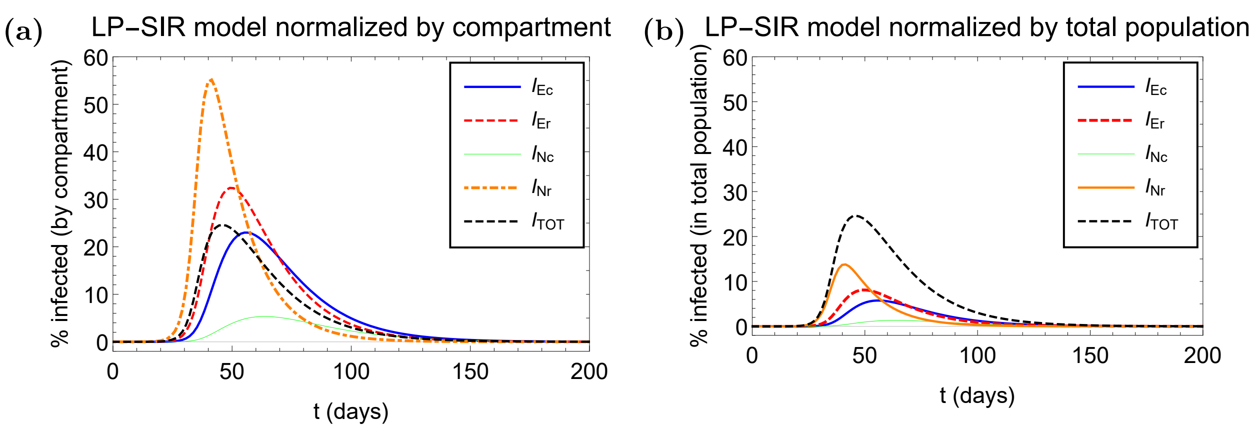

Figure 15: LP-SIR model with even subdivisions of compartments with $\mu = 0.85$. $\alpha_N = 8/24$, $\alpha_E = 1/24$, $\beta_N = 1/24$, $\beta_E = 8/24$ indicating essential (non-essential) workers spend 8 h working at essential (non-essential) locations plus an additional hour at non-essential locations (essential locations). By adding an hour of interaction in non-essential locations, all populations are significantly affected, but have roughly the same peak time (although at different infection peak strengths).

A lockdown of non-essential businesses that accounts for non-compliance can be considered by setting $\alpha_N = 1/24$, $\alpha_E = 1/24$, $\beta_N = 1/24$, and $\beta_E = 8/24$ in the LP-SIR model. This choice reflects a setting in which essential workers perform their usual 8 h shift ($\beta_E = 8/24$). All groups spend 1 h at non-essential locations, reflecting the fact that non-essential workers may still interact with one another, either by ignoring lockdown restrictions or by interacting in crowds outside a business ($\alpha_N = 1/24$, $\alpha_E = 1/24$). $\beta_N = 1/24$ indicates that non-essential individuals must spend some time at essential businesses to satisfy basic needs. The mask compliance was kept at $\mu = 0.85$ to allow comparisons with results in previous sections. Figure 16 shows the infection curves for all compartments using this set of parameters. The dynamics for every compartment are clearly slower than the ones for N_r individuals obtained in all previous simulations in this section. This is reasonable as the effect of a lockdown is to drastically reduce interactions between all non-essential workers at non-essential places (α_N goes from 8 h to 1 h). The fast outbreak for the N_r group seen under no lockdown policies (see Figures 13-15) is no longer present due to the low interaction time of N_r workers at non-essential locations ($\alpha_N = 1/24$), meaning that interactions between individuals within this group were driving the outbreak. In this situation, the population dynamics become dominated by essential workers, as can be expected from the severe restrictions on non-essential interactions that are not applicable to essential workers. These results show that the LP-SIR model can be used as a tool to assess the effect of NPI policies, which is presented in more detail in the next sections.

The two key findings from this section are: interactions at non-essential locations may be responsible for the asymmetry in the infection curves for each subpopulation, and essential workers may play a significant role in the infection dynamics if a lockdown is implemented. These features were observed in the last section as well, where the speed of the infection was associated to the location at which interactions happen. The high peak for the N_r compartment, even under a mask policy suggest that, at the beginning of the COVID-19 pandemic, N_r workers may have driven the infection. The infection curves for essential workers during lockdowns suggests that, during the COVID-19 pandemic outbreak, essential workers may have played an important part in driving the

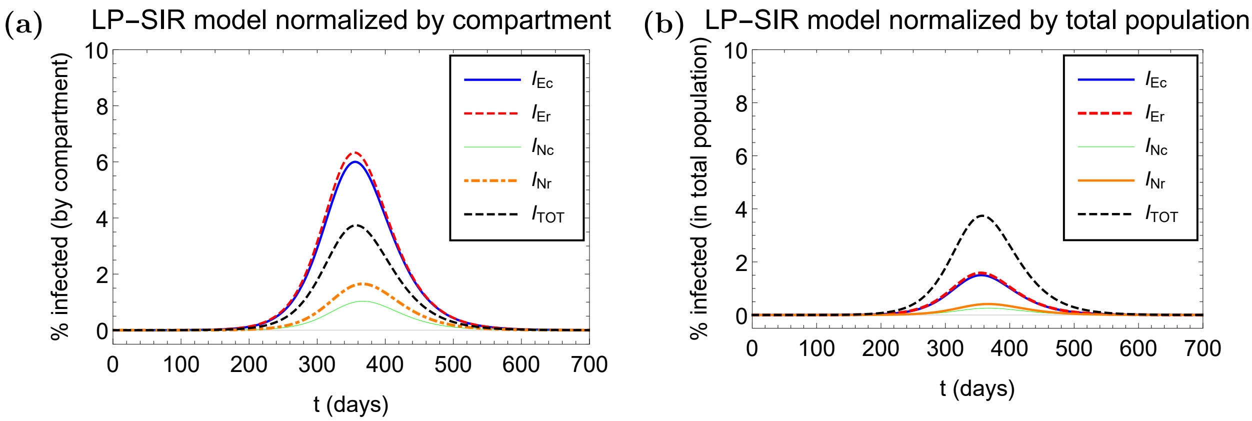

Figure 16: LP-SIR model with even subdivisions of compartments with $\mu = 0.85$. $\alpha_N = 1/24$, $\alpha_E = 1/24$, $\beta_N = 1/24$, $\beta_E = 8/24$ modelling a realistic lockdown in which essential workers keep their usual shift at essential locations. All groups interact 1 h at non-essential locations and non-essential workers spend 1 h at essential locations. The resulting dynamics for N_r are slower than without lockdown, indicating the effectiveness of the policy on that population group. However, contagions of essential workers remain high.

infection during the periods at which lockdowns were imposed.

3.4 Assessing the efficacy of mask and lockdown policies with the LP-SIR model

A critical feature of the LP-SIR model is the incorporation of parameters that model two NPIs: mask mandates on essential businesses and lockdowns at non-essential locations. In the last section, we gained some insight by considering the case of an imperfect lockdown, which resembles a realistic scenario. This section focuses on understanding the effect of different sets of policies in the dynamics of the disease. Throughout this section the initial conditions were fixed as $I_0 = 10^{-6}$ for all groups and the recovery rate was set to $\delta = 1/14\ 1/days$. The infectivities were taken as in the previous section: $\gamma_r = 15.68$ and $\gamma_c = 0.627$. We considered a population of 75% cautious individuals and an even division between essential and non-essential workers.

3.4.1 Mask mandates at essential locations under no lockdown

Mask policies are one of the easiest NPIs to implement as a response to an outgoing outbreak when the disease is airborne. Beyond individual inconvenience, there is minimal economic impact on the population due to mask usage. Facemask are considered to be efficient to prevent the transmission of airborne infectious diseases, but effectiveness on protection for the wearer is still disputed [34], [24]. In a real situation, the efficiency depends on factors as the type of mask, the fit, and most importantly on compliance with the policy [35]. In this part, we consider the overall influence of compliance with mask usage on the outbreak using the LP-SIR model. The compliance level was varied to understand how the dynamics change, and to infer if the subpopulations that drive the infection change for different μ.

Each of the Figures 17-19 show the resulting infection curves, normalized both by compartment and by the total population, when varying the compliance levels to $\mu = 0\%$, $\mu = 50\%$, and $\mu = 95\%$, with the other parameters held fixed ($\alpha_N = 8/24$, $\alpha_E = 1/24$, $\beta_N = 1/24$, and $\beta_E = 8/24$). This choice simulates a scenario in which there is a mask mandate, but no lockdown policy has been set. By comparing the extreme cases in which no mask is used by anyone ($\mu = 0$) with universal mask usage ($\mu = 95\%$), it is clear that this model predicts that compliance with the mask policy has a strong influence on the outcome of the outbreak for essential workers and N_c workers. It also predicts that its impact on the N_r compartment is minimal compared to the impact on other groups. This result is reasonable, as the mask policy only works at essential locations, thus, ensuring

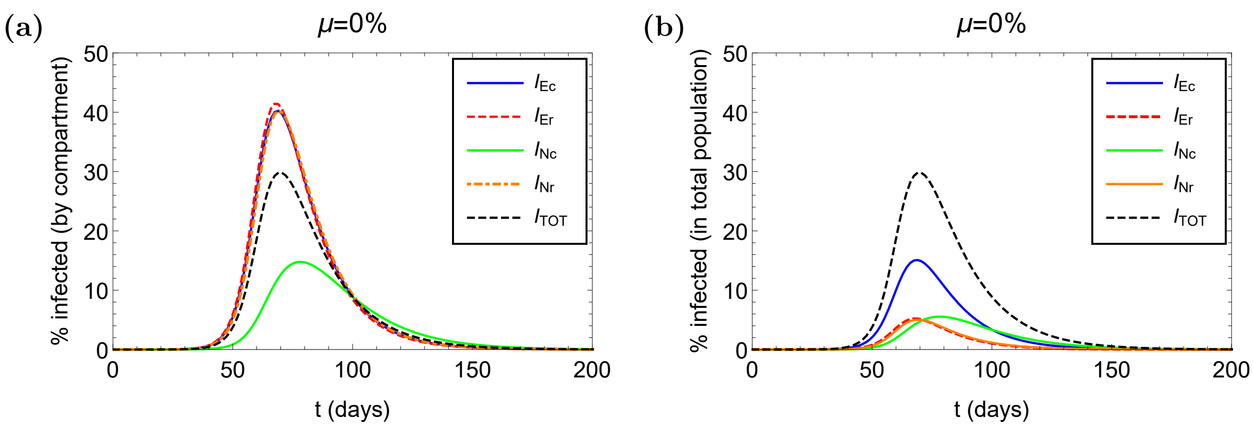

Figure 17: Infection curves normalized by a) each compartment, and b) the total population, for the case of imposed mask mandate but no lockdown policy($\alpha_N = 8/24$, $\alpha_E = 1/24$, $\beta_N = 1/24$, and $\beta_E = 8/24$) for a compliance $\mu = 0$. The dynamics show that the N_r, E_r and E_c have high peaks at nearly the same times, but it is the E_c group that drives the infection due to the size of cautious compartments. This is expected when no risky person wears a mask.

a homogeneous mixing with low (high) infection risk when there is a low (high) mask compliance.

N_r workers, instead, in this scenario interact 8 h at non-essential places and 1 h at essential places. Their higher hazard, thus, comes from interactions at non-essential locations, where they only meet other risky people.

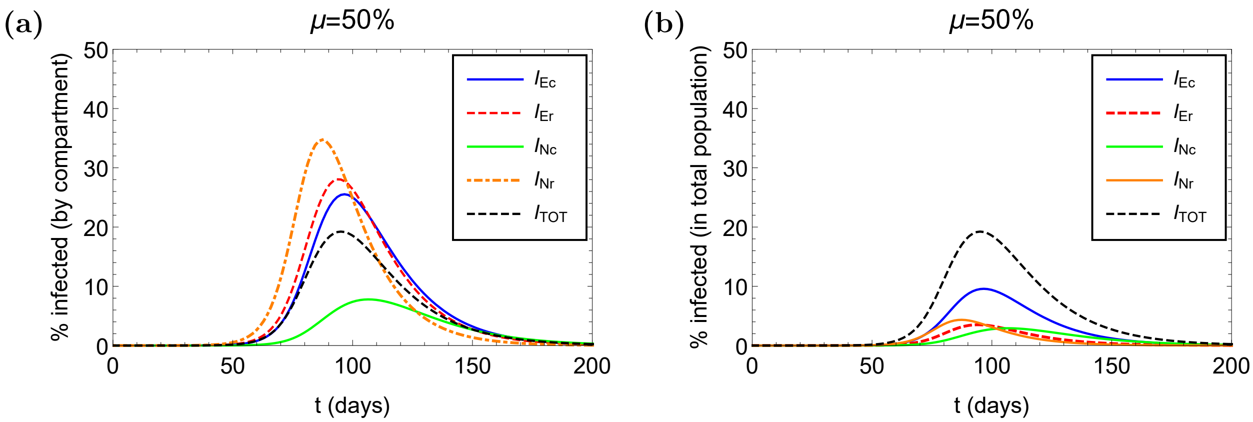

Figure 18: Infection curves for the case of imposed mask mandate but no lockdown policy($\alpha_N = 8/24$, $\alpha_E = 1/24$, $\beta_N = 1/24$, and $\beta_E = 8/24$) for a compliance $\mu = 50\%$. It can be seen in a) that essential workers have their peak decreased and delayed thanks to the increase in compliance, but the E_c group is still the main driver of the disease.

The plots that are normalized by the total population indicate the populations that drive the disease. For $\mu = 0$ (Figure 17) the disease is mainly driven by the E_c group. As μ increases, the infections in N_r start taking over as the main driver of the outbreak. When universal mask usage is reached (Figure 19) the N_r group becomes the main driver of the disease but there is still some influence from essential cautious workers, which indicates that essential workers benefit from a high compliance with the mask mandate. This has been suggested previously in [36]. Finally, notice that the LP-SIR model predicts a benefit not only for essential workers but also for the population as a whole, shown as a fourfold reduction in the peak for the total population when comparing the scenarios for no mask usage and universal mask usage. Hence, our model predicts a mask policy to be effective in reducing infections and avoiding a scenario in which more than half of the population is simultaneously infected (as in the classic SIR model under no interventions). However, the peak with universal mask usage is still around 7%, which is still too high. This indicates that a mask mandate alone may not prevent an outbreak, it may only reduce its adverse effects.

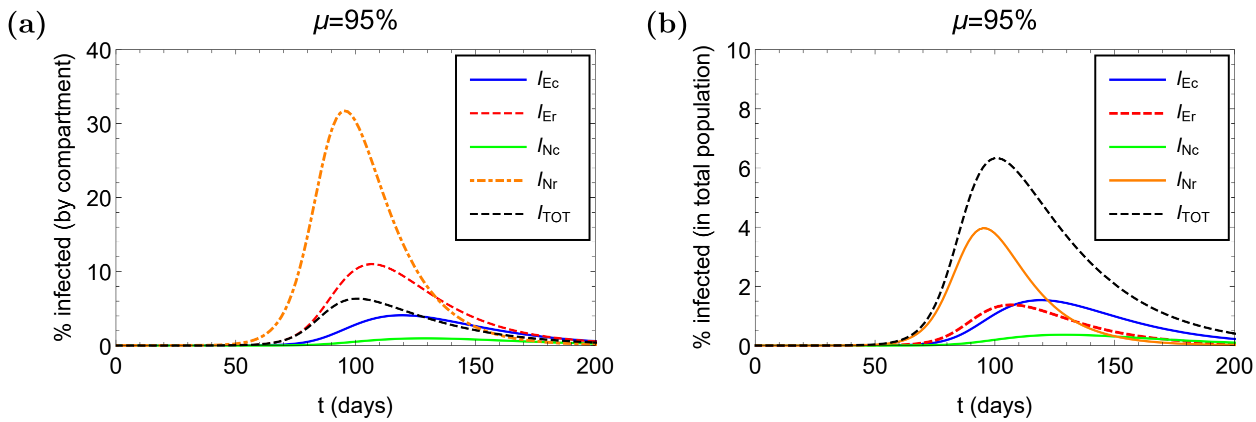

Figure 19: Infection curves for the case of imposed mask mandate but no lockdown policy($\alpha_N = 8/24$, $\alpha_E = 1/24$, $\beta_N = 1/24$, and $\beta_E = 8/24$) for a compliance $\mu = 95\%$. When universal mask usage is reached, the N_r group becomes the main driver of the disease, whereas essential workers have drastically reduced their peaks compared to no mask usage (Figure 17). This indicates that mask mandates affect essential workers and N_c in a higher degree. The peak for the total population is around 7%, which is still too high and suggests that mask policies alone are unable to prevent an outbreak but serve to limit its adverse effects.

3.4.2 Lockdown at non-essential locations under no mask policies

Mask usage is not the only approach to prevent an outbreak. Another policy that has been commonly implemented is a lockdown of non-essential workers. In the LP-SIR model, lockdowns of different types can be considered thanks to the spatial structure, which provides two kind of locations: essential and non-essential locations. In this section, lockdowns at non-essential locations without a simultaneous mask mandate are considered. In this way, it is possible to decouple the effect of lockdowns from that of mask policies. This is important because the economic impact of lockdowns is much bigger than the one for mask mandates.

A lockdown at non-essential locations can be modeled by reducing the time-interaction parameters α_N and α_E, while keeping $\beta_N = 1/24$ and $\beta_E = 8/24$ fixed. A partial lockdown can be thought of as an scenario in which α_N and α_E are reduced 50%, whereas a total lockdown is represented by choosing $\alpha_N = 0 = \alpha_E$. Figures 20 and 21 show the dynamics for scenarios in which a partial lockdown and total lockdown for non-essential locations were implemented, but no mask policy was in place. The dynamics for the case in which no lockdown was imposed ($\alpha_N = 8/24$,

$\alpha_E = 1/24$, $\beta_N = 1/24$, and $\beta_E = 8/24$) was already shown in Figure 17, where a large infection curve is obtained for all but the N_c compartment. If α_N and α_E are sequentially reduced, the biggest benefit is for the N_r compartment for the same reason discussed before: interactions at non-essential locations for risky people involve a high risk due to assortativity.

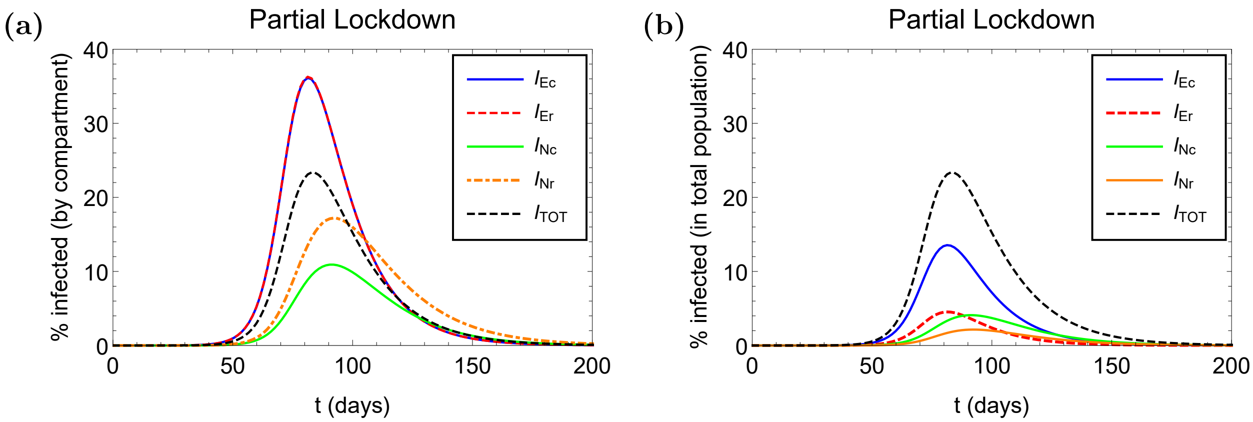

Figure 20: Infection curves for the case of a partial lockdown policy ($\alpha_N = 4/24$, $\alpha_E = 1/48$, $\beta_N = 1/24$, and $\beta_E = 8/24$) with no mask mandate ($\mu = 0\%$). By comparing this to Figure 17, it is clear that a partial lockdown affects mainly to the N_r compartment. The main driver of the disease is the $E_c group$, suggesting that essential workers may play a significant role in the infection when lockdowns are in place.

By comparing Figures 17 and 21, it can be seen that a reduction of more than 30% in the infection peak for N_r workers is achieved due to the lockdown. The peak for essential workers, however, does not change significantly, with a reduction of less than 6% in the peak. This follows from the nature of essential workers jobs: even under a lockdown policy, they must keep working at their usual workplaces. The reduction in the infection peak for the total population under a total lockdown policy at non-essential locations is around 10%, compared to a reduction of nearly 30% under universal mask usage found in the previous part. In fact, if one focus on essential workers, it can be seen that there is almost no reduction in their peaks when lockdowns at non-essential locations are implemented, they always drive the infection. It follows that, according to the LP-SIR model, implementing a lockdown policy at non-essential locations alone is not an effective strategy if it is not coupled with a mask mandate. Interestingly, though, a lockdown at non-essential locations benefits the compartment for which the mask policy was almost irrelevant, the non-essential risky

(N_r). This provided two key insights: i) Essential workers may be an important reservoir for the infection if a mask policy is not present, and ii) A better outcome may be achieved by combining mask and lockdown policies together, which we explored next.

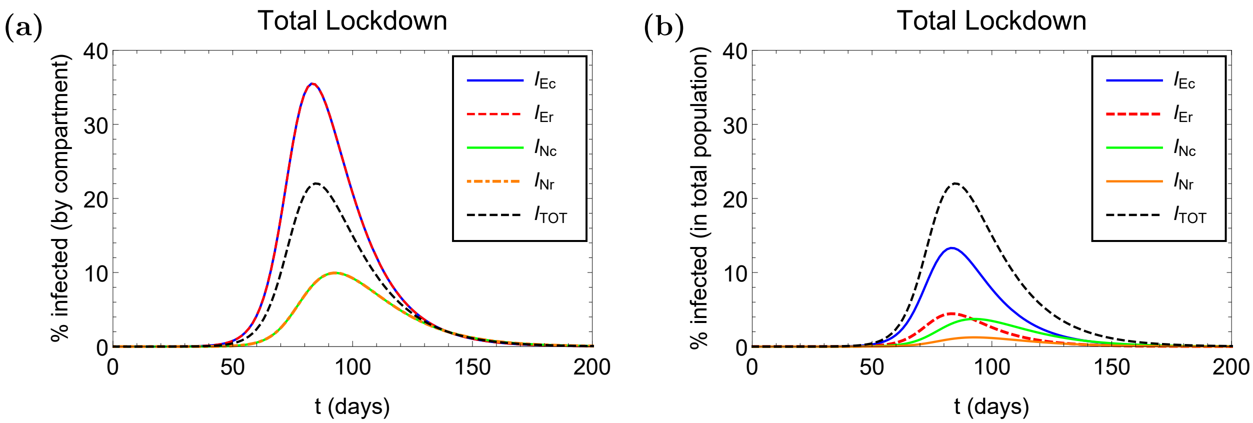

Figure 21: Infection curves for the case of a total lockdown policy ($\alpha_N = 0$, $\alpha_E = 0$, $\beta_N = 1/24$, and $\beta_E = 8/24$) with no mask mandate ($\mu = 0\%$). There is further reduction in the peak for the N_r group, but the essential workers infections remain almost invariant. This confirms that lockdowns at non-essential locations affect N_r individuals to a higher degree, and it suggests that essential workers may be an important reservoir of the infection when there are lockdowns but no mask policies in place.

3.4.3 Lockdown at non-essential locations under a mask mandate at essential locations

In this section, the effect of simultaneously applying a mask mandate at essential locations with a lockdown policy at non-essential locations is considered. We studied the cases of a partial lockdown where mask compliance is 75% and 95% and the case of a total lockdown at a mask compliance of 85%. In the case of the partial lockdown, it was found that a 75% compliant mask policy would not suffice to prevent an outbreak but would reduce its intensity and delay it, which is shown in Figure 22. More interestingly, by combining the partial lockdown with universal mask usage, the LP-SIR model predicts that there would not be an outbreak, as it is shown in Figure 23. By comparing this to Figure 20, the effect of combining the two policies revealed astonishing. It is clear that the peaks for all populations are strongly reduced, and that there is a large delay for the peak to occur, shifting from around $t = 60$ days to $t = 550$ days. If a total lockdown at non-essential locations

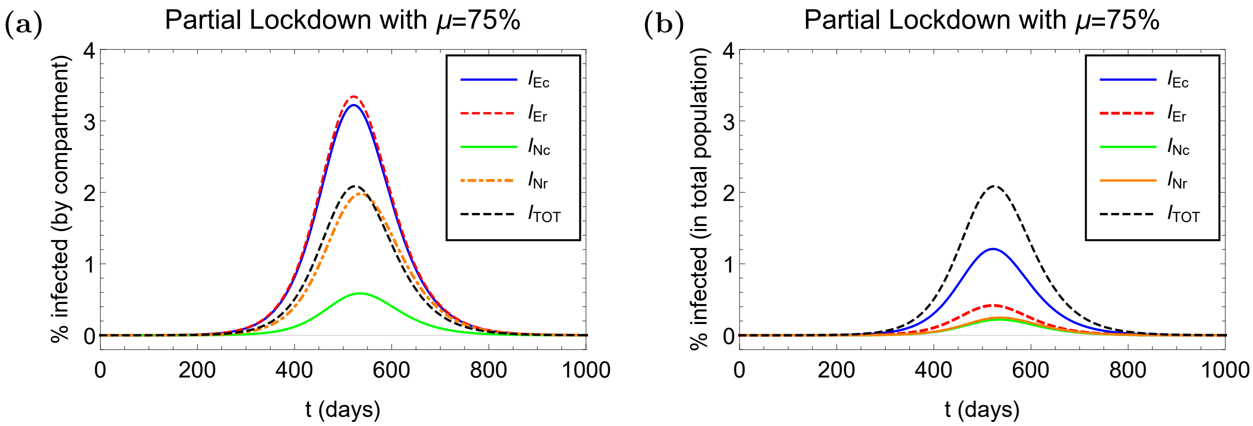

Figure 22: Infection curves for the case of a partial lockdown policy ($\alpha_N = 4/24$, $\alpha_E = 1/48$, $\beta_N = 1/24$, and $\beta_E = 8/24$) with a mask mandate where $\mu = 75\%$ of individuals are compliant. The dynamics show that this combination of policies is insufficient to prevent an outbreak, but it serves to decrease the peak and delay it for more than a year, which would buy precious time until pharmaceutical interventions become available.

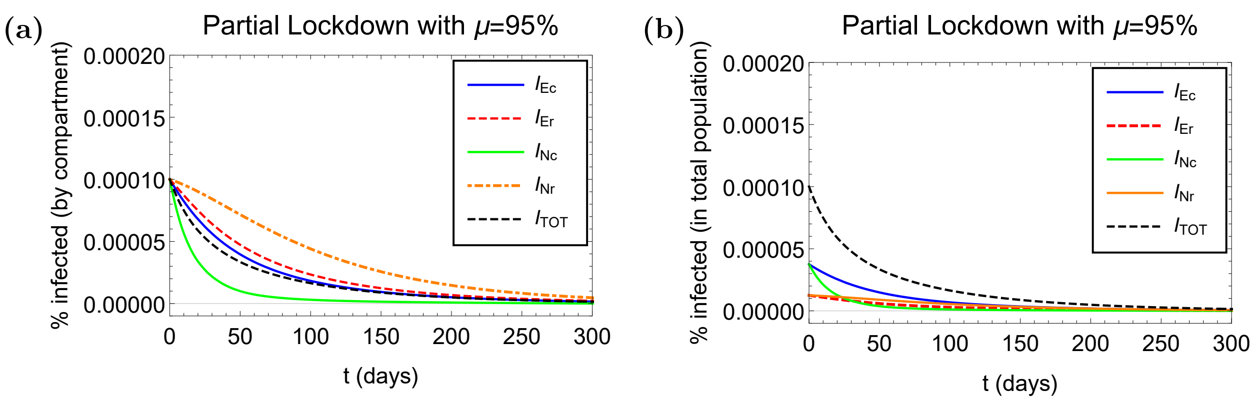

Figure 23: Infection curves for the case of a partial lockdown policy ($\alpha_N = 4/24$, $\alpha_E = 1/48$, $\beta_N = 1/24$, and $\beta_E = 8/24$) with a mask mandate where $\mu = 95\%$ of individuals are compliant. This result is encouraging as it suggests there is a threshold for mask compliance at which it would be possible to prevent an outbreak without requiring total lockdowns.

is applied, the compliance needed to prevent an outbreak reduces to $\mu = 85\%$, as it is shown in Figure 24.

At first sight, these results seem encouraging, since they suggest that if mask compliance is high enough, total lockdowns might not be necessary. However, it is important to emphasize that this result assumes that masks provide 80% of outward protection and that policies are constant

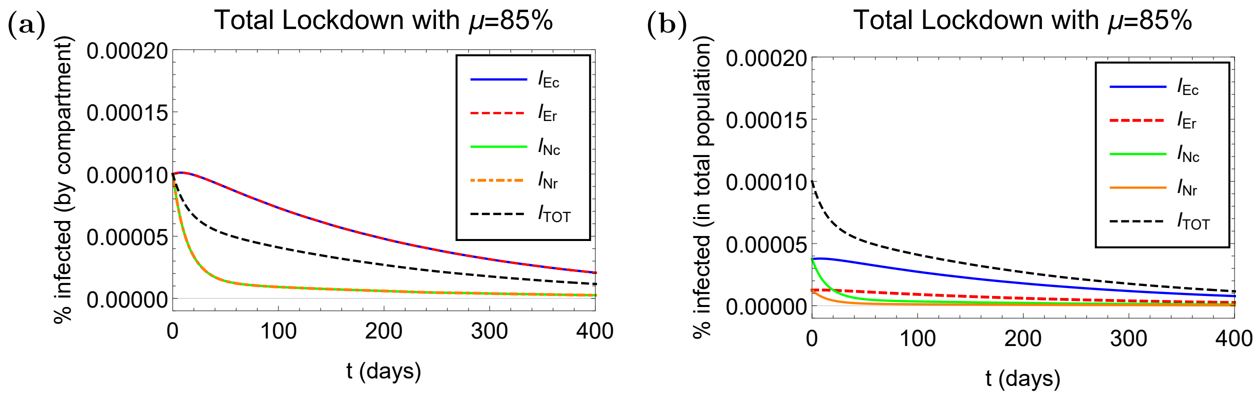

Figure 24: Infection curves for the case of a total lockdown policy ($\alpha_N = 0/24$, $\alpha_E = 1/48$, $\beta_N = 1/24$, and $\beta_E = 8/24$) with a mask mandate where $\mu = 85\%$ of individuals are compliant. This result suggests that there is a trade-off between the levels of mask compliance and the degree of lockdowns needed to prevent an outbreak. A fundamental assumption is that policies are set up from the beginning of the infection, which is relaxed in next section.

over time. That is, in order to prevent an infection, the policies must have been present since the beginning of the infection. In addition, the outcome depends on the ratio between essential/non-essential populations and cautious/risky, which would have to be adapted to the specific local community, and it would also depend on the specifics of the disease (γ, δ, etc.).

The main result from this section is that by combining a lockdown policy at non-essential locations with a mask mandate at essential locations, it may be possible to prevent an outbreak without requiring a total lockdown. There are, however, conditions on the values of mask compliance, the percentage of essential workers and the percentage of risky individuals. There is a trade-off between these values in determining the outcome of an outbreak. For the case of a total lockdown, the infection is dominated by essential workers, so increasing the fraction of essential workers increases the number of infections over time. This can be compensated either by reducing the fraction of risky workers in the population or by increasing the mask compliance. For the case of a partial lockdown, the infection is driven by the non-essential risky compartment. In this case, increasing the fraction of essential workers in the population decreases the infections, since risky individuals must wear masks at essential locations, reducing the likelihood of spreading the disease. A similar interplay occurs if we consider other diseases with different basic reproduction numbers

R_0, indicating that our model could be applied for a variety of diseases for which the conditions to prevent an outbreak could be identified.

3.5 Effect of time dependence in the effectiveness of policies

One of the limitations in the previous results is that the parameters modeling lockdowns and mask mandates are kept constant over time. This served to model policies that went into effect as soon as infections started. This constraint, however, is unrealistic as people's reaction to an imposed policy and policies themselves vary over time. By allowing time dependence for the time interaction parameters (α_N, α_E, β_N, and β_E) and the mask compliance (μ), the aim was to understand the effect of the timing of lockdown and mask mandate policies onto the dynamics of an infectious disease. In particular, the interest was to understand the influence of late adoption of lockdowns and mask policies into the dynamics, and also to discern if there is still a benefit for the population in spite of late adoption. In this section, we built on results from the previous section by modifying the model to include temporal dependence for the parameters. Logistic functions were used to simulate the changes in policies and/or the behavior of the population in response to them, with $\alpha_N(t) = \sum_i a_i f((t - t_i)/\tau_i)$.

The effect of late adoption of a mask policy at essential locations was analyzed to account for the delay between the enactment of the policy and its adoption. The mask policy is assumed to be implemented at essential locations by the government at a certain day after the initial infections were detected. It is also assumed to be quickly adopted by the population. We considered the same scenario as in Figure 22 (a partial lockdown for non-essential workers from the beginning of the outbreak) but with the mask policy adopted 35 and 60 days after the initial cases. These choices reflect the timeframe it took for most local governments in the US to implement a mask policy. The maximum compliance was set to 75%, reached a few days after the policy was enacted. Figure 25 show the results for a delay of 35 days. It can be seen that the infection happens a lot earlier, but the peak is negligibly higher than in the case in which the mask policy was set from the start. If the delay for setting up the mask policy is 60 days, which is shown in Figure 26, the infection

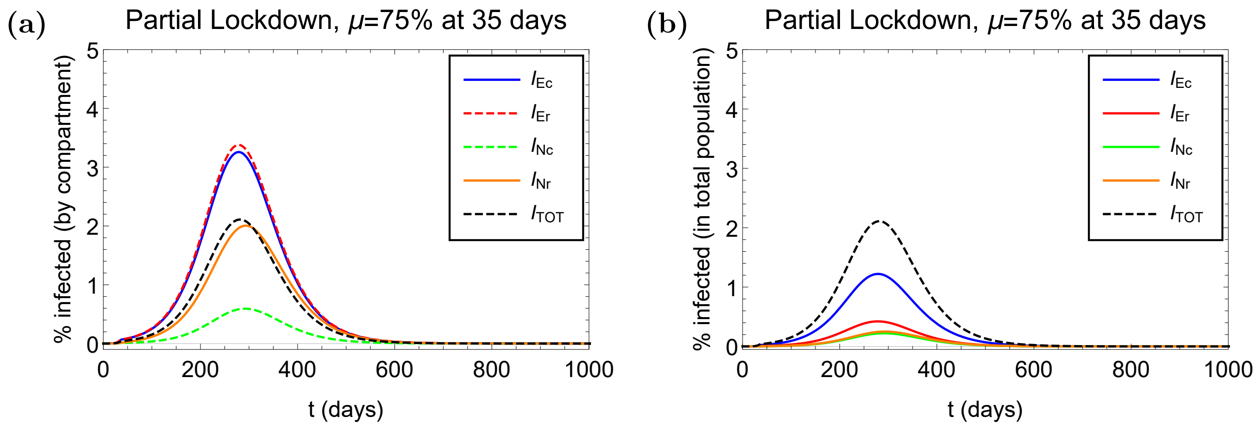

Figure 25: Infection curves for the case of a partial lockdown policy ($\alpha_N = 4/24$, $\alpha_E = 1/48$, $\beta_N = 1/24$, and $\beta_E = 8/24$) with a mask mandate that is delayed for 35 days and reaches a compliance of $\mu = 75\%$. By comparing this to Figure 22, it can be seen that the peak happens a lot earlier (almost half of the time), but it is only negligibly higher. This indicates that delaying the enactment of the mask policy worsens the infection by making it faster.

happens even earlier, and the peak almost duplicates in value. This highlights the importance of the mask policy: the timing and the level of compliance could heavily influence the prevalence of the infection. Notice that essential workers drive the infection in both cases, which is consistent with our previous findings because a partial lockdown decreases the infections in compartments involving non-essential workers, whereas infections for essential workers increase during the period where a mask policy is absent.

An important remark is that for any given disease, there is a characteristic timescale dictated by both the infectivity and the recovery rate, which are often encompassed in the effective reproduction number (R_0). Accordingly, if the characteristic timescale of the disease is shorter than the delay period, no effect will be seen due to the delay. Conversely, if the timescale of the disease is larger than the delay period, there will be an exponential increase in the infection. That is, during the delay period, the dynamics will be in agreement with the evolution of the outbreak under no interventions.

The effect of late adoption of a lockdown policy at non-essential locations was also analyzed. The lockdown policy is assumed to be implemented by the government at a certain day after the initial infections were detected. It is also assumed to be quickly adopted by the population

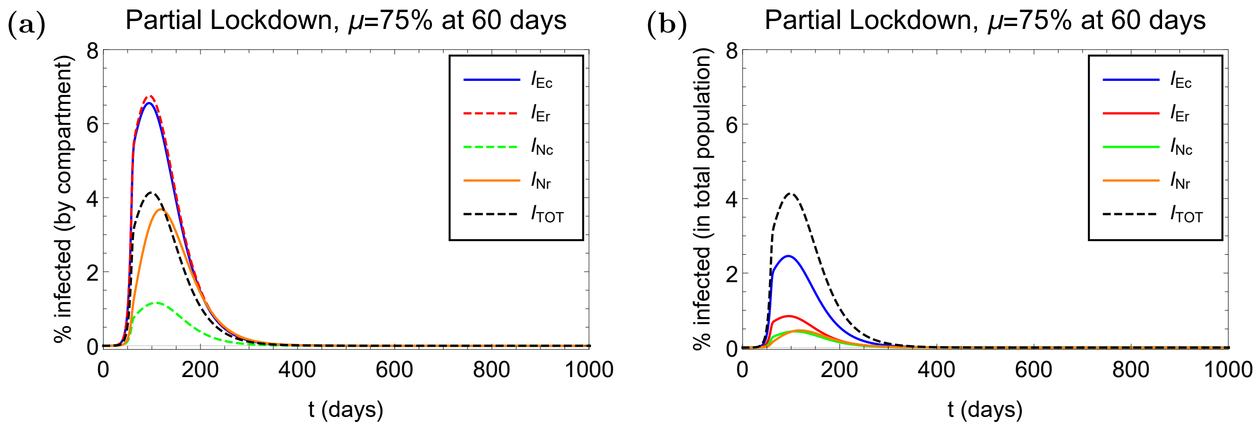

Figure 26: Infection curves for the case of a partial lockdown policy ($\alpha_N = 4/24$, $\alpha_E = 1/48$, $\beta_N = 1/24$, and $\beta_E = 8/24$) with a mask mandate that is delayed for 60 days and reaches a compliance of $\mu = 75\%$. By comparing this to Figures 22 and 26, it is clear that the peaks happen a lot earlier and almost double in value. This suggests that both the timing of and the level of compliance with the mask policy heavily influence the dynamics of the infection.

ending in a total lockdown scenario. Previously, it was found that for a total lockdown policy, 85% compliance resulted in no outbreak (see Figure 24). Figure 27 shows the results when the total lockdown policy is delayed for 60 days from the first infections. As it can be seen, the infections in the non-essential risky group (N_r) grow until the lockdown policy is imposed. Thus, a delay in setting up the lockdown policy results in larger infections for the N_r group. If the mask compliance is low, this can function as a precursor of a bigger infection as members of the N_r group spread it to other groups at essential locations. This is consistent with our previous findings that a lockdown especially affects to non-essential risky workers.

The results in this section suggest that even delayed NPIs offer substantial benefits for the population. Nevertheless, the benefit decreases for longer delays. This indicates that the timing of the policies is also a crucial factor to consider when an outbreak is ongoing. Our results also suggest that by combining focused lockdowns for non-essential workers with a mask mandate at essential locations, it may be possible to control an infectious disease and prevent an outbreak given that the facemasks provide enough protection, compliance with the policies is high and the policies are implemented in a timely manner.

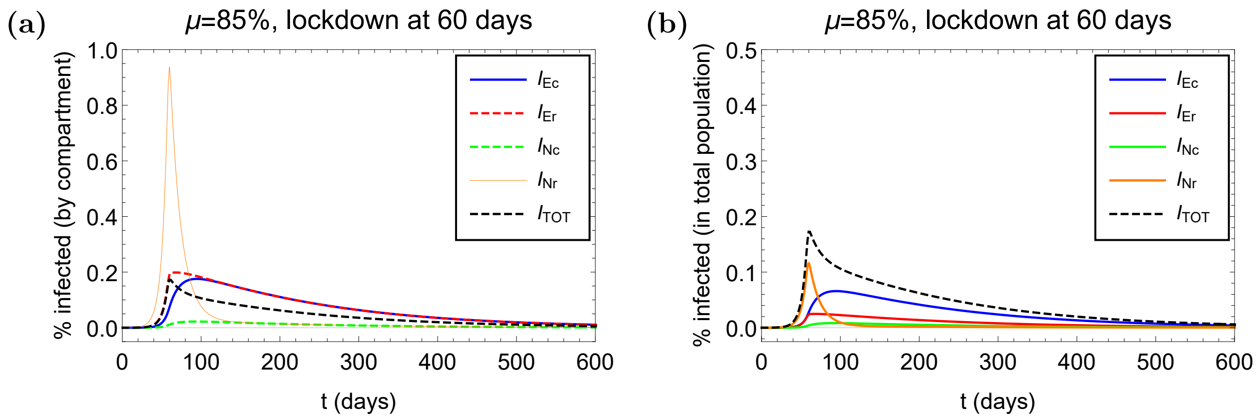

Figure 27: Infection curves for the case of a total lockdown policy ($\alpha_N = 0$, $\alpha_E = 0$, $\beta_N = 1/24$, and $\beta_E = 8/24$) that is delayed for 60 days and a mask mandate with $\mu = 85\%$ compliance. The dynamics clearly show that delaying the lockdown policy exacerbates the infection in the N_r group, which is consistent with our previous results indicating that lockdowns affect primarily to N_r workers (see Figures 20 and 21). The high peak for the N_r compartment, when the lockdown policy is delayed suggest that, at the beginning of the pandemic, N_r workers may have driven the infection, as lockdown policies were not implemented immediately after detecting the first cases.

3.6 Assessing the LP-SIR model with real data

A direct way of assessing the performance of the LP-SIR model in real infections would be to use mobility data structured according to whether a worker is essential or not. However, we were unable to find this type of data, so we resorted to an indirect assessment by estimating the time spent by non-essential workers at non-essential locations. Replacing the time spent at non-essential locations α (a constant) with $\alpha(t)$ (a function of time) gives a continuous degree of freedom, which would allow any infection dynamics to be recovered.

In this section, the gradient descent algorithm was applied to the SIR model to determine the infectivity that would best fit real infection curves at the beginning of the pandemic, where NPI policies were not yet implemented. We also used a set of times $\{t_i\}$ that correspond to policy decisions enacted in disparate regions of the US (specifically Texas, California, and New York) to shape $\alpha_N(t)$. By fitting the observed infection statistics in these regions to a time-varying mobility $\alpha_N(t)$, we demonstrate the LP-SIR model can be applied to real world data (as can potentially be true for any infection model). We use this fitting to infer the elevated hazard experienced by essential workers in each of these regions. The time-interaction parameters for essential locations, $\beta_N(t)$ and $\beta_E(t)$ were inferred from Walmart's reduced hour policy [37], which is summarized in Table 1. Both functions were modeled as shown in Figure 28 using logistic functions $\beta(t) = \sum_i b_i f((t-t_i)/\tau_i)$.

Table 1: Timeline for Walmart reduced hour policy for most of their retail stores [37], which was used to define $\beta_N(t)$ and $\beta_E(t)$

Policy	from	to
Reduced hours to 11.5h	March 19, 2020	August 14, 2020
Reduced hours to 13h	August 15, 2020	November 13, 2020
Reduced hours to 14h	November 14, 2020	-
Mask policy for employees	April 20, 2020	-
Mask policy for shoppers	July 20, 2020	-

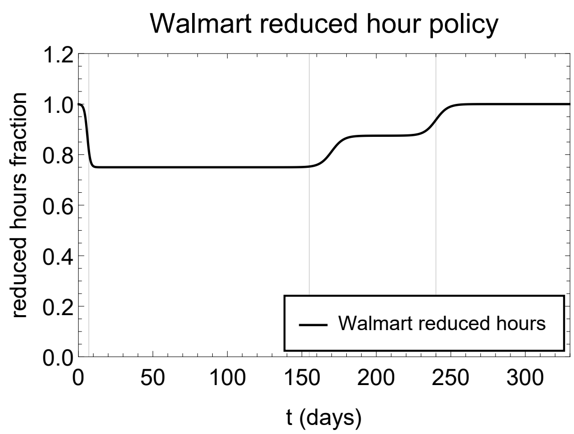

Figure 28: Walmart reduced hours policy implemented due to COVID used to define $\beta_N(t)$ and $\beta_E(t)$.

3.6.1 Extracting the infectivity rate from the New York infection curve

We first used real data for CoVID-19 active infections extracted from ref. [12]. The state of New York (NY) was selected to find the value of the infectivity and compare it with the value we used for the classic SIR model. Choosing NY follows from the timeline at which NPI policies were implemented by the government. At NY, the first case was detected in March 1st, 2020. The first request to social distance and avoid densely packed areas came in a week later. The first closures began 15 days after the first case was found, whereas the first lockdown policies were implemented 21 days later. Given these considerations, we chose to treat the first 10 days on infections at NY using the classic SIR model to extract the value for the infectivity under no implemented policies. These assumptions are reasonable since within those 10 days, the government was deciding which are the right measures to implement and people were still adopting a corresponding behavioral response, so the expectation of a well-mixed homogeneous population should hold.

The gradient descent algorithm was used to generate a best fit for the infectivity of a classic SIR model. The resulting value was $\gamma_{opt} = 4.0954$ with an error of the order of 10^{-6}. Figure 29 shows the fitted curve and the infection data for the state of New York, which shows the same exponential growth as the real infection, but overlooks fluctuations and other stochastic effects that give raise to the small deviations. As we discussed before when presenting results for the classic SIR model this is consistent with the averaging effect due to the coarse assumptions of this model.

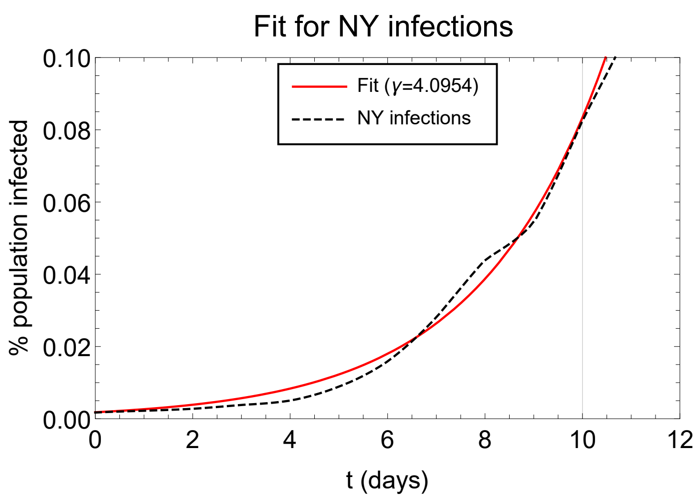

Figure 29: Real infection curve for the state of New York. The gradient descent algorithm using an SIR model was applied to find the infectivity that generates a best fit during the timeframe when no interventions were in place, which correspond to a classic SIR model. The best fit value resulted $\gamma = 4.0954$, which closely matches previously reported data. The small deviations are due to heterogeneity, fluctuations and stochastic effects that are overlooked by the classic SIR model

3.6.2 Using the LP-SIR model to extract mobility data for non-essential workers

Mobility data at non-essential locations for non-essential workers was extracted using the LP-SIR model from real infection curves for three states within the United States: New York, Texas, and California. Mask usage was extracted from [12]. The initial conditions were extracted from [12] and the ratios cautious vs risky and essential vs non-essential were extracted from data provided by [38] for New York, [39] for California and [40] for Texas. The recovery rate was 1/14 $1/days$ (a 2 week recovery period) as in previous sections. The infectivity for risky individuals was calculated as a weighted average of a population composed of 65% of cautious individuals and 25% of essential workers. The resulting infectivity was $\gamma_r = 31.9$. As in previous sections $\gamma_c = 0.04\gamma_r = 1.28$, which indicates that cautious individuals have a lower probability of transmitting the disease than risky ones due to their mask usage.

We originally intended to utilize mobile phone data [41], [42], [12] to model the mobility of the non-essential compartment, but we found that the data suggested an *increase* in mobility before lockdown policies were relaxed. In other words, there was an increase in the mobility of New Yorkers during the most restrictive lockdown according to [12]. We thus decided to use non-essential mobility as a fitting parameter, given the timing of local lockdown policies. To find the mobility for non-essential workers at non-essential locations, $\alpha_N(t)$, the gradient descent algorithm was applied to minimize the error between a real infection curve and the output of the LP-SIR model. We used logistic functions centered at specific times at which a policy affecting the mobility of non-essentials workers was imposed, that is, with the same structure as before: $\alpha_N(t) = \sum_i a_i f((t - ti)/\tau_i)$. Replacing α (a constant) with $\alpha(t)$ (a function of time) gives a continuous degree of freedom, which would allow any infection dynamics to be recovered. In this section, we will focus on a set of times $\{t_i\}$ that correspond to policy decisions enacted in disparate regions of the US (specifically Texas, California, and New York). By fitting the observed infection statistics in these regions to a time-varying mobility $\alpha(t)$, we demonstrate the LP-SIR model can be applied to real world data (as can potentially be true for any infection model). We use this fitting to infer the elevated hazard experienced by essential workers in each of these regions. The initial amplitudes and strengths for the logistic functions were manually selected and later optimized using a gradient descent algorithm. Figure 30 shows the results for the state of New York. By comparing this mobility data with the imposed policies shown in Table 2, it can be seen that there is a correlation between the types of policies that were implemented and increases/reductions in non-essential mobility at non-essential locations.

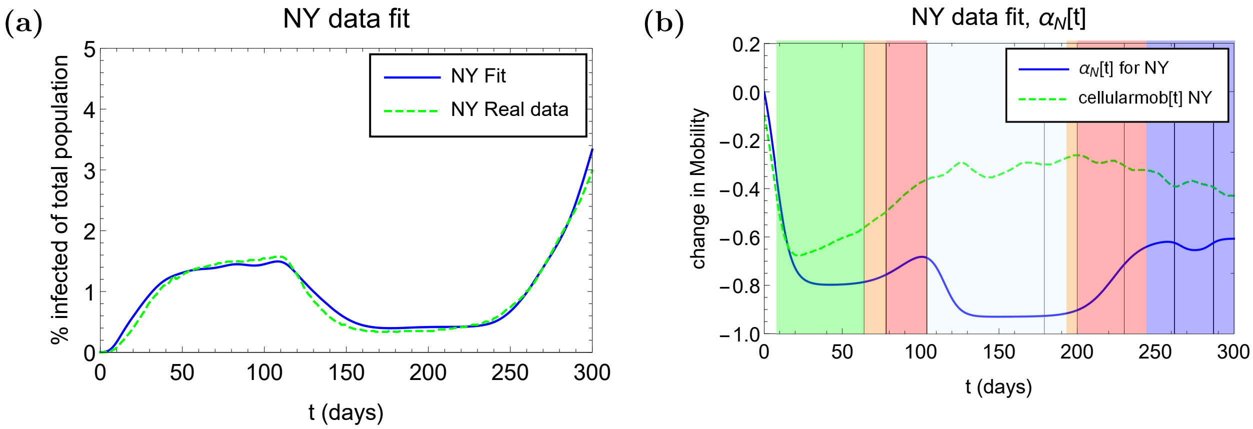

Figure 30: a) Fit to real NY infection curve using a gradient descent algorithm and initial conditions for the centers of the logistic functions manually set. b) Resulting non-essential workers mobility at non-essential locations $\alpha_N(t)$ and cellularmob(t) showing real mobility data extracted from [12]. Background colors indicate the expected effect of the policy in the mobility. Green indicate strict measures, including lockdown, closures, and limitations on gatherings. Orange indicates some measures begin to be relaxed. Red indicates further relaxation of policies. Light blue represents a travel advisory requiring travelers to self-quarantine. Blue indicates schools turned all operations remote and suspension of interior dine-in.

Table 2: Timeline of applied policies at New York

Policy	from	to
Reduced mobility recommendations	March 7, 2020	March 22, 2020
Lockdown on non-essentials	March 22, 2020	May 15, 2020
Non-essential gatherings forbidden	March 24, 2020	May 31, 2020
Relaxed lockdown	May 29, 2020	June 16, 2020
Further relaxations	June 2, 2020	June 23,2020
Travel advisory	June 24, 2020	October 31, 2020
Restaurants at 75%	September 17, 2020	-
Non-compliant businesses closed	October 23, 2020	November 11, 2020
No indoor dine-in	December 14, 2020	-

Based on the $\alpha_N(t)$ extracted using the LP-SIR model, we can potentially use the dynamics to infer the subpopulations that are driving the disease at any point in time. Figure 31 shows that essential workers drive the disease during various periods and act as a reservoir during others. This is consistent with what was found in previous sections, and it likely results from the interplay of low mask usage (for the first period) and the increase in mobility (for the last peak). This also indicates that differentiating between essential and non-essential workers in reported infection data could provide an important pathway to controlling or preventing the outbreak. Previously, we concluded that lockdown policies do not have a strong impact on essential workers and that mask policies do not have a strong impact on non-essential risky workers. Given that these subpopulations are driving the disease, a higher mask compliance at the beginning might have reduced the first peak, whereas maintaining a lower mobility might have prevented the latest increase in infections.

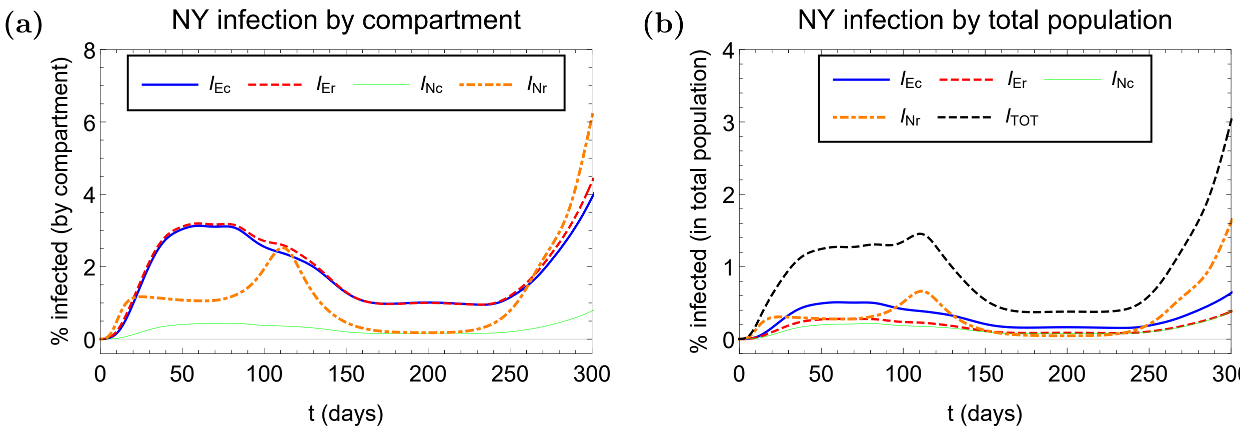

Figure 31: a) Infections for the E_r, E_c, N_r, and N_c compartments normalized by subpopulation in NY state, which show that essential workers are more affected than non-essentials within their own communities. b) Same as in a) but normalized according to the total population. Non-essential workers drive the disease at the beginning, at the middle and at the end of the timeline, when mobility of non-essential workers at non-essential locations increases.

It is also possible to estimate whether or not a given subpopulation is at an increased risk compared to others by calculating the ratio between infections. In this way, we found that essential workers are exposed to a higher hazard throughout the infection, except for brief periods of time. In the literature, it has been suggested that essential workers may be exposed to a higher risk due to work-related system-level failures [19]. Figure 32 shows comparisons for the essential vs non-essential subpopulations and for the cautious vs risky subpopulations. The risky subpopulation drives the disease almost exclusively, except for a brief period of time (around 170-230 days). Similarly, essential workers drive the disease except for a 3-week period at the beginning of the outbreak and a 1-week period around 290 days.

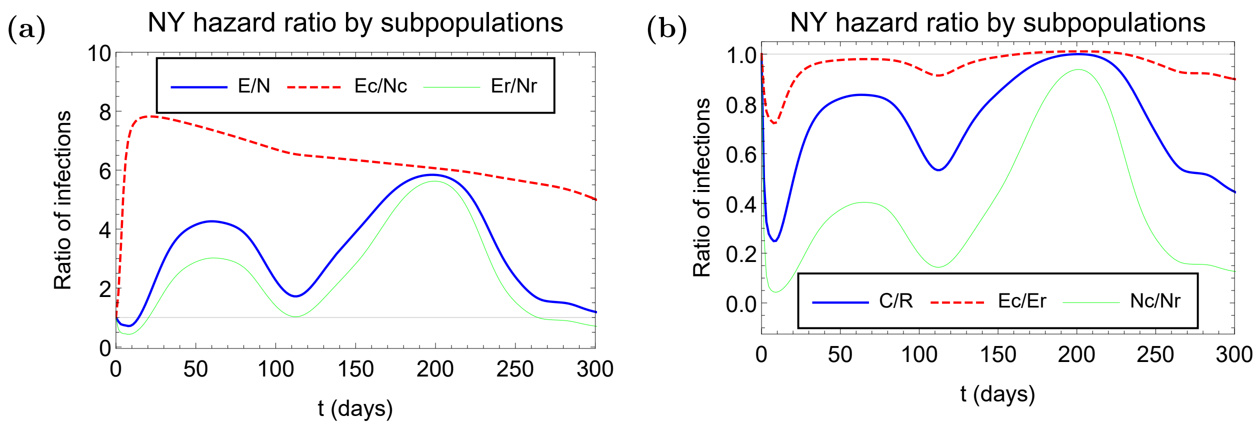

Figure 32: a) Hazard ratio of essentials vs non-essential workers at NY. It is shown that essential workers drive the disease most of the time, except at the beginning and at the end. b) Hazard ratio of the cautious vs risky subpopulations at NY. It is shown that risky individuals drive the disease in most of the shown timeline.

A similar procedure was followed for the states of Texas and California, as shown in Figures 33-36. Results mimic the behavior observed for New York with a main difference: the first peak on the infection is not present anymore. This is likely due to mobility restrictions imposed coupled with less infected individuals in the population ($I_0 = 10^{-6}$ for TX, $I_0 = 5 \times 10^{-6}$ for CA,$I_0 = 2 \times 10^{-5}$ for NY) and the provision of PPE for essential workers as well as the tax removal on PPE for CA. Also, non-essential risky workers drive the infection only during the first period at which measures were relaxed. In NY, N_r workers always drove the infection. This suggests that it may be important to ensure that enough compliance with the mask policy has been achieved prior to relaxing lockdown measures. During the period of first relaxations mask compliance was $56 - 75\%$ for TX and $67 - 78\%$ for CA [12], which may have not been enough to prevent transmission from non-essential risky individuals to essential workers.

Results for TX are shown in Figures 33-35. By using Table 3 and the color coding in Figure 33, notice that there is a correlation between imposed policies and increases or decreases in mobility except for the last period after 250 days. Beyond these 250 days, pharmaceutical interventions, including the newly distributed vaccinations affected the number of infections, as they were not as high as it would be expected from the imposed policies.

Texas started with the lowest number of infections; thus, it is possible that lockdown policies

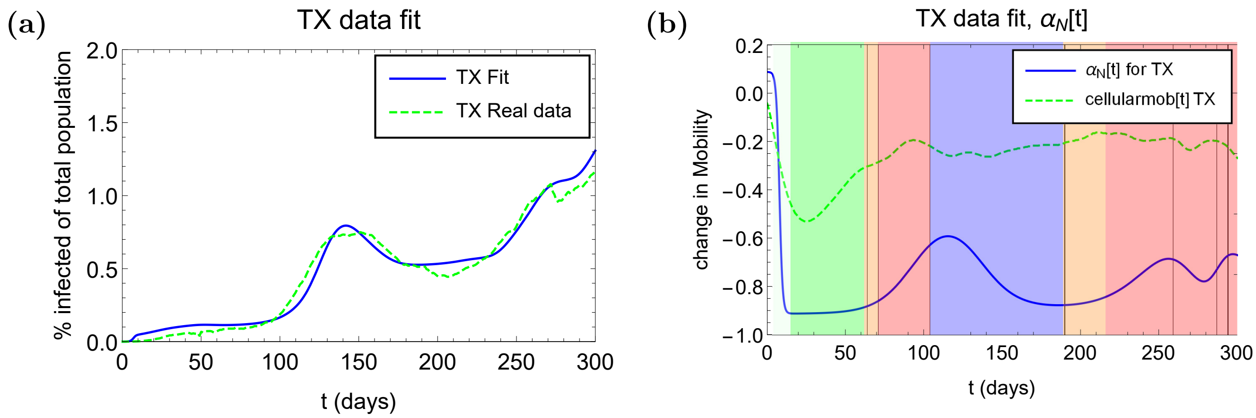

Figure 33: a) Fit to real TX infection curve using a gradient descent algorithm and initial conditions for the centers of the logistic functions manually set. b) Resulting non-essential workers mobility at non-essential locations. Background colors indicate the expected effect of the policy in the mobility. Green indicate strict measures, including lockdown, closures, and limitations on gatherings. Orange indicates some measures begin to be relaxed. Red indicates further relaxation of policies. Blue represents stricter measures put back in place.

Table 3: Timeline of applied policies at Texas

Policy	from	to
Bar closures, no dine-in	March 16, 2020	March 31, 2020
Stay home order	March 24, 2020	April 30, 2020
Wedding, personal care reopen	May 6, 2020	May 8, 2020
Further reopening	May 22, 2020	June 23, 2020
Stricter measures back in place	June 24, 2020	September 17,2020
Restaurants at 75%	September 17, 2020	-
Bars reopen at 50%	October 14, 2020	-

managed to inhibit infections for non-essential risky workers, explaining why infections in the N_r compartment die out after an initial increase. Conversely, infections for essential workers never decrease, which may be explained by an insufficient value of mask compliance in the first stage of the outbreak. During the period of relaxation of lockdown policies, non-essential risky individuals drive the infection, which in turn increases the infection for essentials. This is consistent with the dynamics of the infection shown in Figure 34. Figure 35 shows the hazard ratios for cautious vs risky and essential vs non-essential. In this case essential workers drive most part of the infection as well, with brief periods in which essential risky workers drive the infection. These periods are related to relaxation of imposed policies.

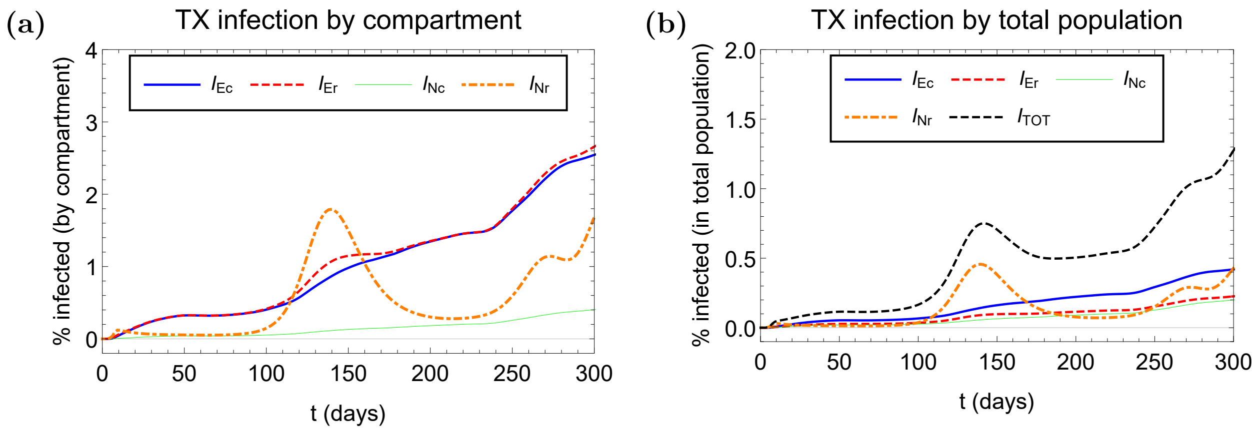

Figure 34: a) Infections for the E_r, E_c, N_r, and N_c compartments normalized by subpopulation in TX, which show that essential workers are more affected than non-essentials within their own communities except at the middle of the infection curve. b) Same as in a) but normalized according to the total population. Non-essential workers drive the disease at the only at the middle, when mobility of non-essential workers at non-essential locations increases due to relaxation in policies.

We then reproduced the computations for the state of California, which resulted in very similar trends than the infection in Texas, but with a higher percentage of infected population. This is likely due to a higher number of initially infected individuals than in TX (but still lower than in NY). The gradient descent fit and the extracted mobility $\alpha_N(t)$ are considered in Figure 36. Again, by matching this mobility to the policy timeline for the state shown in Table 4, it can be seen that there is good agreement between policy changes (inception and relaxation) and non-essential mobility at non-essential locations. Since, there are no significant differences in the dynamics for subgroups and the hazard ratios, they were omitted.

Table 4: Timeline of applied policies at California

Policy	from	to
Call for bars' closures	March 15, 2020	-
Lockdown on non-essentials	March 19, 2020	May 15, 2020
1st stage reopening	May 8, 2020	June 30 ,2020
Ban on indoor services	Jul 1, 2020	August 31, 2020
Stricter measures reimposed	November 16, 2020	-

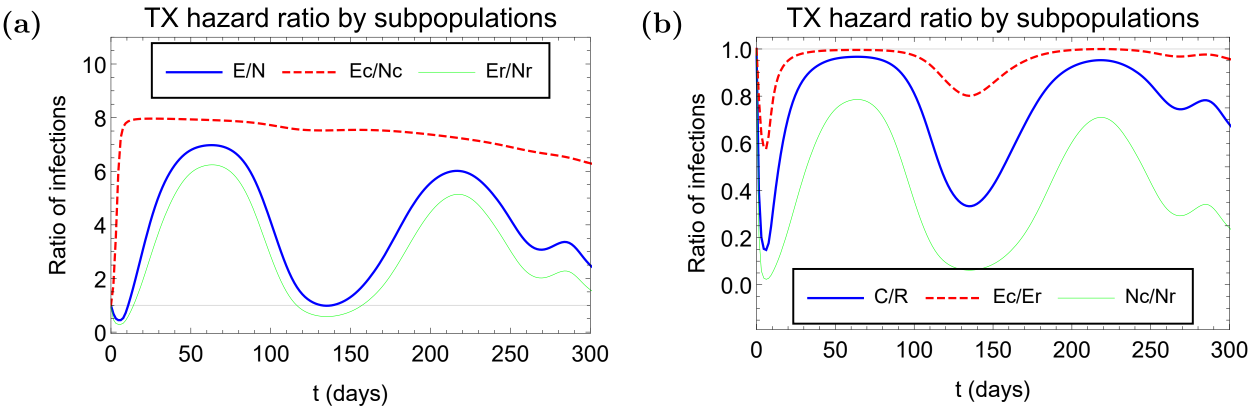

Figure 35: a) Hazard ratio of essentials vs non-essential workers at TX. It is shown that essential workers drive the disease most of the time, except at a brief period in the middle of the outbreak. b) Hazard ratio of the cautious vs risky subpopulations at TX. It is shown that risky individuals always drive the disease.

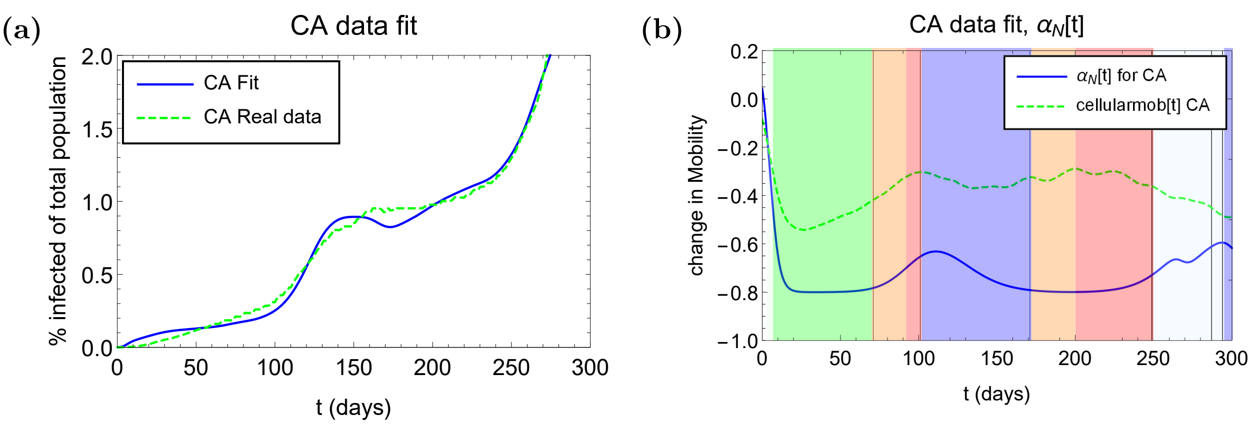

Figure 36: a) Fit to real CA infection curve using a gradient descent algorithm and initial conditions for the centers of the logistic functions manually set. b) Resulting non-essential workers mobility at non-essential locations. Background colors indicate the expected effect of the policy in the mobility. Green indicate strict measures, including lockdown, closures, and limitations on gatherings. Orange indicates some measures begin to be relaxed. Red indicates further relaxation of policies. Blue represents stricter measures put back in place.

It is important to emphasize that, in this section, we are assuming that all essential workers (or non-essential workers) behave and interact in the same way within a community, which is not extrictly valid in a whole state due to the differences between cities or countryside and metropolis (e.g. when we applied the LP-SIR model to TX, NY and CA). We are also assuming that all essential workers (even for different cities within a state are well-mixed), which is clearly not true. Data for active infections at county level is available, but other information, such as policies implemented in a specific county or the mask compliance by county is harder to get. These approximations hide out some details about heterogeneity of the population by averaging them over each state. By obtaining data for all time-dependent parameters at the county level and using the LP-SIR model to get predictions about the outbreak in each community, the performance of the LP-SIR model could be better assessed.

4 Transmission between heterogeneous neighborhoods with LP-SIR model

Results from previous sections indicate a difference in the dynamics of infection when subpopulation sizes are changed. One key insight was that essential workers are an important reservoir for the infectious disease during the lockdown periods due to their disproportionately high interaction time compared to non-essentials workers. In this section, we consider a model with two heterogeneous neighborhoods. Neighborhoods were labeled as Heavily Essentials-Neighborhood (HEN) and Heavily Non-Essential Neighborhood (HNN) to facilitate the discussion. The former is composed mainly of essential workers and the latter is mainly inhabited by non-essential workers. The structure of the LP-SIR model was maintained in both neighborhoods, with an assumption that the populations within neighborhoods preferentially interact within their neighborhood. This is an additional level of assortativity in the model, consistent with the behavior observed in social networks [43]. We continue to assume an assortativity within the cautious and risky subpopulations in each community. The assortativity within a neighborhood is broken for essential workers that must commute from one neighborhood to the other for their required jobs. In this section, we assume that one neighborhood has a greater number of essential workers while the other neighborhood has a greater number of essential jobs. This may be a plausible representation of low-income neighborhoods commuting to wealthier neighborhoods to perform essential jobs.

In this section, we considered a series of simplifying hypothesis. The main assumption was that only a fraction of essential workers commutes between neighborhoods to go to their workplace. This is a reasonable approximation since most people commute from home to work on a daily basis and prefer to live close to their workplace (if economically possible). The second assumption is that essential workers live day to day and cannot afford to switch jobs suddenly. A third assumption is that the non-essential population is composed mainly of individuals that can work remotely or can switch jobs to one that allows it. Combined, these assumptions imply that the categories of essential vs non-essential workers in each neighborhood are fixed during the pandemic, and the only possibility of infection between the two neighborhoods is through the essential workers commuting between neighborhoods.

4.1 Transmission of an outbreak starting at Heavily Essential Neighborhoods

A scenario in which the disease starts at a Heavily Essential Neighborhood (neighborhood 1) and transmits to a Heavily Non-Essential Neighborhood (neighborhood 2), was considered by choosing a set of parameters as shown in Table 5. All compartments except for the commuters have an initial fraction of infected people 10^{-5}. The time interaction parameters were chosen to reflect a lockdown at non-essential locations: $\alpha_E = 0 = \alpha_N$, $\beta_N = 1/24$, $\beta_E = 8/24$, the mask compliance was $\mu = 0.85$, the recovery rate was 1/14 $1/days$, and the effective infectivity $\gamma_r = 31.9$, as in the previous section. The results are shown in Figure 37. Clearly, the infection happens for all groups at HEN, whereas at HNN it only happens for commuting essential workers that travel to HEN ($E_{2\to1}$) and get infected there. This indicates that under a lockdown at non-essential places (where non-essential workers are only allowed 1 h for shopping essentials), the disease is transmitted between neighborhoods only through $E_{2\to1}$ workers. Both subgroups, $E_{2\to1,c}$ and $E_{2\to1,r}$, are interacting at essential locations, so their dynamics show the expected homogeneous mixing.

Table 5: Parameters for neighborhoods transmission simulations

Neighborhood	% essentials	% risky	% commuters	$\frac{I_0}{S_0}$(non-commuter)	$\frac{I_0}{S_0}$(commuter)
HEN	80	35	25	10^{-5}	0
HNN	10	35	25	0	0

We further considered lockdowns at non-essential locations targeted only to either essential workers (case 1) or non-essential workers (case 2). In case 1, where essential workers are not allowed at non-essential locations ($\alpha_E = 0$), we found that increasing α_N affects only non-essential groups at HEN, with the N_r group affected to a higher degree. For $\alpha_N = 8/24$, the peak in infections for the N_r group is almost doubled compared to the one for $\alpha_N = 0$, whereas it increases in less than 4% for N_c. The infections for essential populations are almost invariant with the increase in α_N. These results are shown in Figure 38. In this situation, it is clear that the N_r group drives the

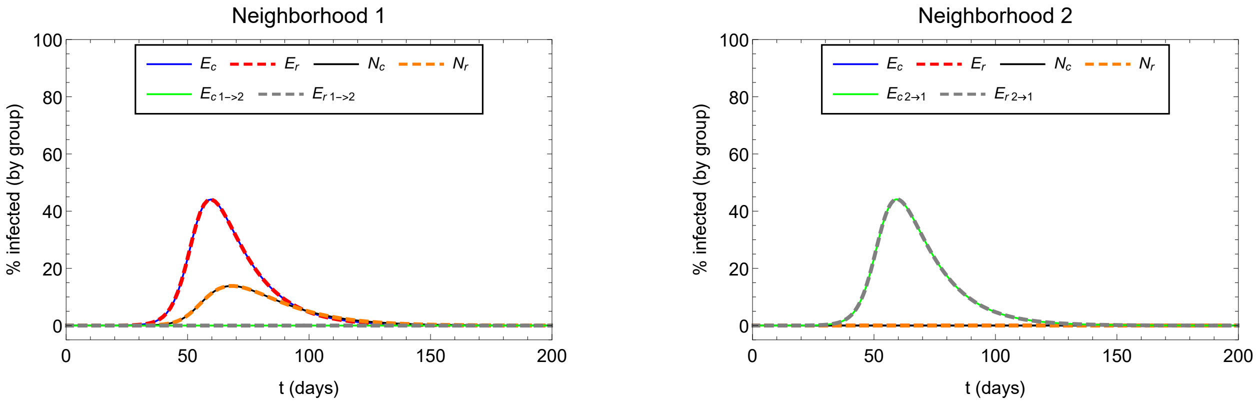

Figure 37: Infection curves at the two neighborhoods when infections start at HEN, with $\alpha_N = 0$, $\alpha_E = 0$, $\beta_N = 1$, $\beta_E = 8$. If essential workers are not allowed to interact at non-essential locations, spread at HNN neighborhood is limited to commuters.

infection at HEN alongside essential workers. In the HNN, the infection is still driven by essential commuters only. In case 2, where non-essentials are banned from non-essential locations, however,

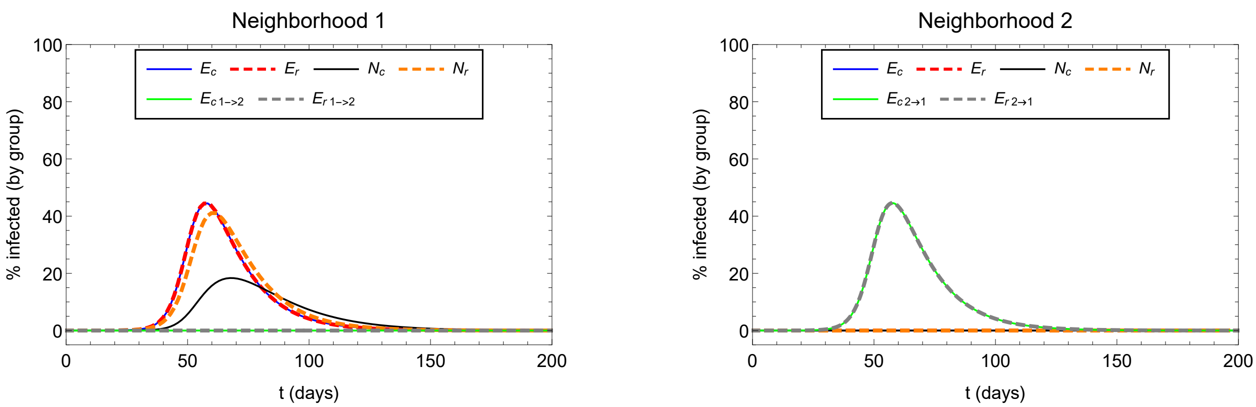

Figure 38: Infection curves at the two neighborhoods when infections started at HEN, with $\alpha_N = 8$, $\alpha_E = 0$, $\beta_N = 1$, $\beta_E = 8$. If essential workers are not allowed to interact at non-essential locations, spread at HNN is limited to commuters. By increasing α_N, the only noticeably increase in infections happens for non-essentials compartments at HEN. HNN groups are almost unaffected.

a minor increase of α_E from 0 to 1/24 already causes infections for all HNN non-commuters. Thus, at HNN, initially, the infection is carried by workers commuting to HEN. It then spreads through contacts at non-essential locations and causes an outbreak for all HNN populations. These results are shown in Figure 39. In this case, it is obvious that essential workers drive the infection at both neighborhoods.

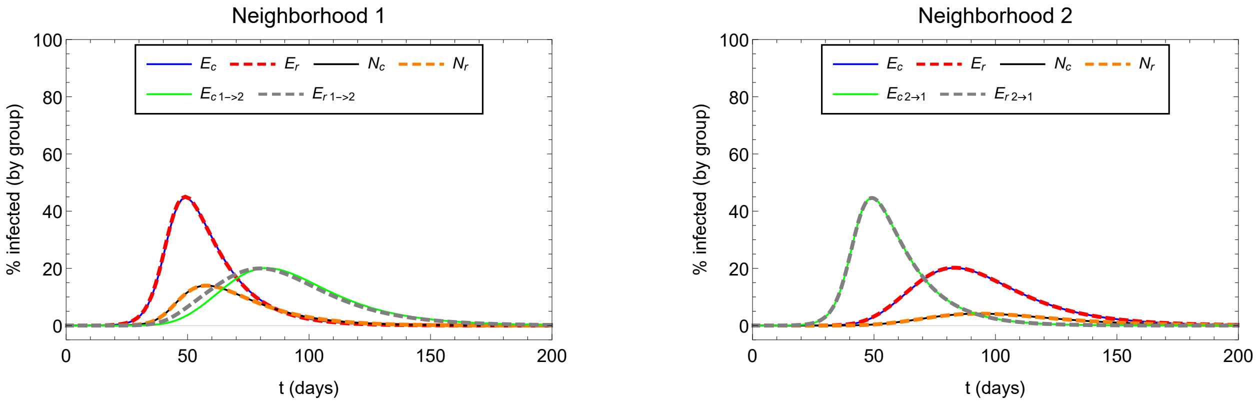

Figure 39: Infection curves at the two neighborhoods when infections started at HEN, with $\alpha_N = 0$, $\alpha_E = 1$, $\beta_N = 1$, $\beta_E = 8$. If essential workers are allowed to interact at non-essential locations, spread at HNN happens for all groups but delayed with respect to infections at HEN.

Size effects make it overly complicated to infer the total infection curve from the data presented above. To understand the effect on the total population, the total infection was calculated by normalizing over the total neighborhood population. Figure 40 shows that under a perfect lockdown ($\alpha_N = 0 = \alpha_E$) the total infection barely hits the HNN. By setting $\alpha_E = 1/24$, there is a noticeable increase in the peak, but there is also a delay. For the scenarios where a perfect lockdown at non-essential locations is applied, at the HNN, infections occur for essential commuters only, which saturates as the corresponding susceptible compartment depletes. Notice that with 10% essential workers and 25% of them commuting, there are only 2.5% of commuters in that neighborhood. When $\alpha_E = 1/24$, however, the infection hits all groups which explains why the peak occurs later, but it is also higher.

A dominant feature in the simulations above is that the dynamics of commuter essential workers resemble that of people working at the same location, that is, non-commuter essential workers. This is the expected homogeneous mixing behavior for interactions at essential locations only, and it remains true as long as essential workers are not allowed to interact at non-essential locations. In the case they are allowed to interact at non-essential locations, that is, $\alpha_E \neq 0$, this symmetry is broken due to the higher risk at which the risky subpopulation is exposed.

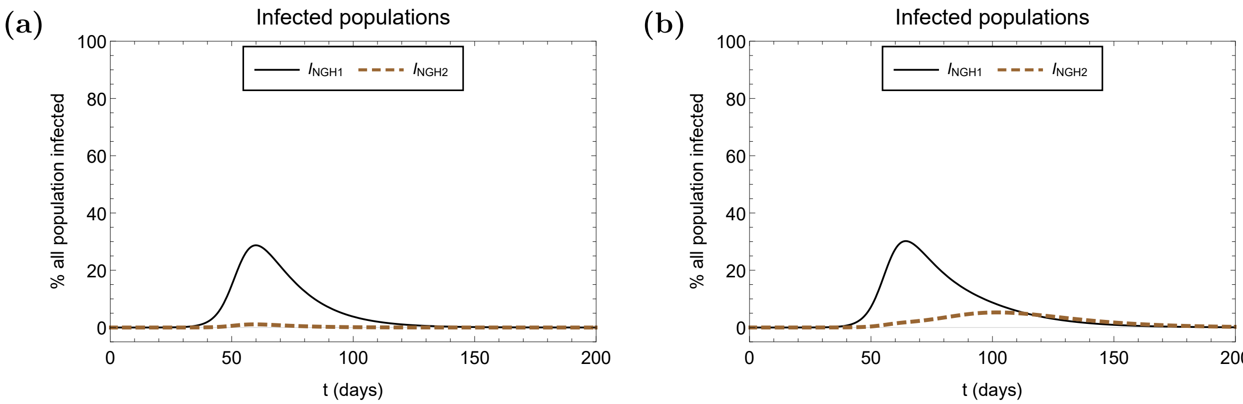

Figure 40: Total infections by neighborhood when the infection starts at HEN and transfers to HNN through commuter workers, with a) $\alpha_E = 0$. b) $\alpha_E = 1/24$. It is clear that changing α_E has negligible effect on the HEN, and a small impact on the HNN.

4.2 Outbreak starting at Heavily Non-Essential Neighborhoods

In this section, we explored the dynamics of an infection that starts at HNN, and transfers to an HEN only through commuters from the HNN. In Figure 41, the results for a perfect lockdown at non-essential locations ($\alpha_N = 0 = \alpha_E$) are presented. The peak is not only delayed but it is also smaller in value than in the case where the disease starts at HEN and transfers to HNN through commuter workers (see Figure 37). This result follows from the smaller number of susceptible essential individuals at HNN compared to HEN. A smaller susceptible population implies there are fewer interactions, which delays the peak of infection.

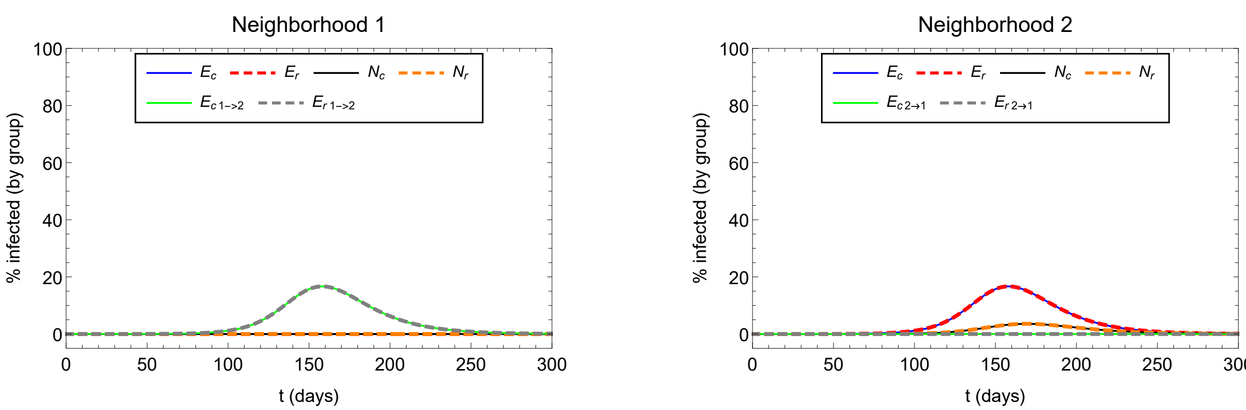

Figure 41: Infection curves at the two neighborhoods when infections started at HNN, with $\alpha_N = 0$, $\alpha_E = 0$, $\beta_N = 1$, $\beta_E = 8$. If essential workers are banned from non-essential locations, spread at HEN is limited to commuters. Infections are lower and delayed than in reverse transmission.

We again considered lockdowns at non-essential locations that are targeted only to either essential workers (case 1) or non-essential workers (case 2). In case 1, if $\alpha_N > 4/24$ (the time spent by non-essential workers at non-essential locations), the peak in the infections for the N_r group surpasses the one for essential workers. This means that the main drivers of the infection are the infected N_r workers. Figure 42 shows the results for $\alpha_N = 3/24$ and $\alpha_N = 8/24$. For $\alpha_N = 3/24$, at HNN, the infections for non-commuting essentials (E_c, E_r) and N_r are balanced, whereas for $\alpha_N = 8/24$ the infections in the N_r compartment dominate over all others. This behavior is the result of the large population size of non-essential workers at HNN. Allowing them to interact at non-essential locations would, thus, cause a larger outbreak driven by essential workers at HEN. At HNN, however, the outbreak is initially driven by N_r workers with essential workers driving the infection later on.

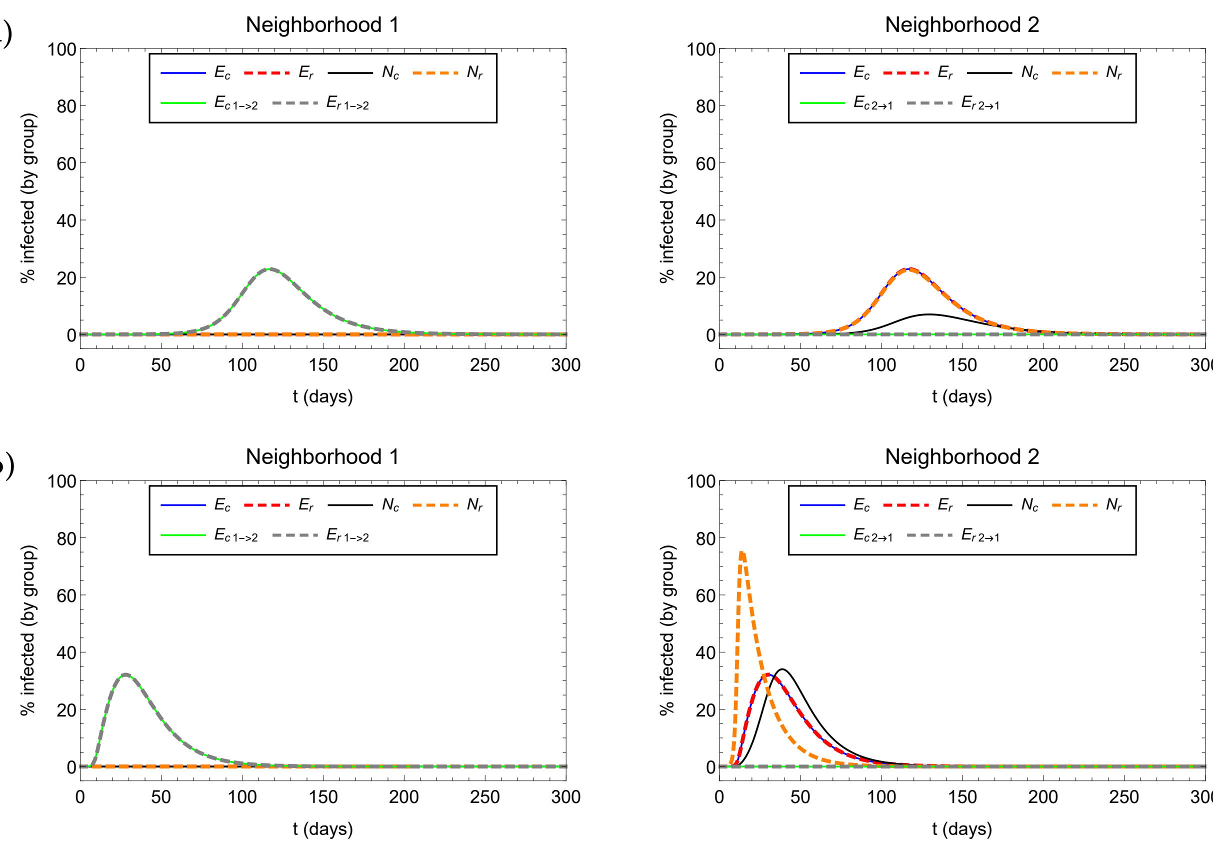

Figure 42: Infections at the two neighborhoods for the cases $\alpha_E = 0$, $\beta_N = 1$, $\beta_E = 8$ and a) $\alpha_N = 3$ and b) $\alpha_N = 8$. The plot shows that as α_N increases, the infections for N_r at HNN become dominant, but essential workers still contribute significantly to the transmission of the disease.

In the previous section, when we analyzed the case 2, where non-essentials are banned from non-essential locations, we found that varying α_E from 0 to 1/24 had a big impact on the dynamics at HEN, causing all groups to have an outbreak. Likewise, if the infection starts at HNN, the functional form of the infection curves remains almost the same as in Figure 39 for all compartments. The only difference is a small delay in reaching the infection peak for all subpopulations. Results are shown in Figure 43. This feature indicates that the timing of the peak depends on the origin of the infection, which suggest again that essential workers may play a major role in the transmission of an infectious disease.

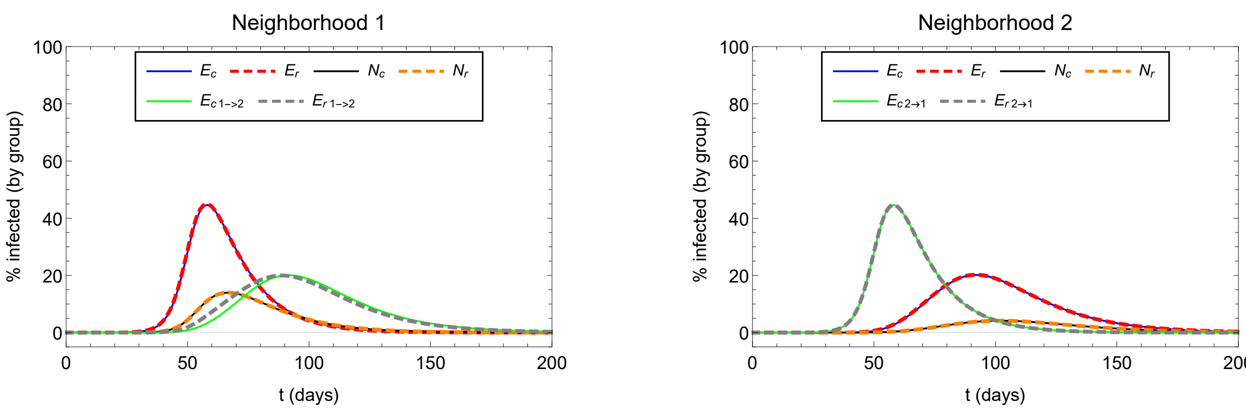

Figure 43: Infections at the two neighborhoods with $\alpha_N = 0$, $\alpha_E = 1/24$, $\beta_N = 1/24$, and $\beta_E = 8/24$. If essential workers are allowed to interact at non-essential locations, spread at an HEN happens for all groups but delayed with respect to an HNN.

To understand the impact of the disease in each neighborhood, it is important to normalize the infections curves with respect to their total population. Results are shown in Figure 44. By comparing this results to the ones in Figure 40, it is clear that if $\alpha_E = 0$, there is a significant outbreak only if transmission goes from an HEN to an HNN, whereas if $\alpha_E = 1$, an HEN is always affected more than an HNN, regardless of where the infection started. Strikingly, even if α_E is set as low as 0.01, the only effect is a delay on the peak but the impact on essential workers remains almost unchanged, as shown in Figure 45. This suggest that in a real situation, where lockdowns are imperfect (and thus $\alpha_E > 0$) the population of an HEN is at a greater risk of contracting the disease due to their intrinsic composition. This also suggests that perfect compliance with a lockdown policy is needed from essential workers in order for it to be effective, which confirms that they may have a significant role in the transmission of infectious diseases.

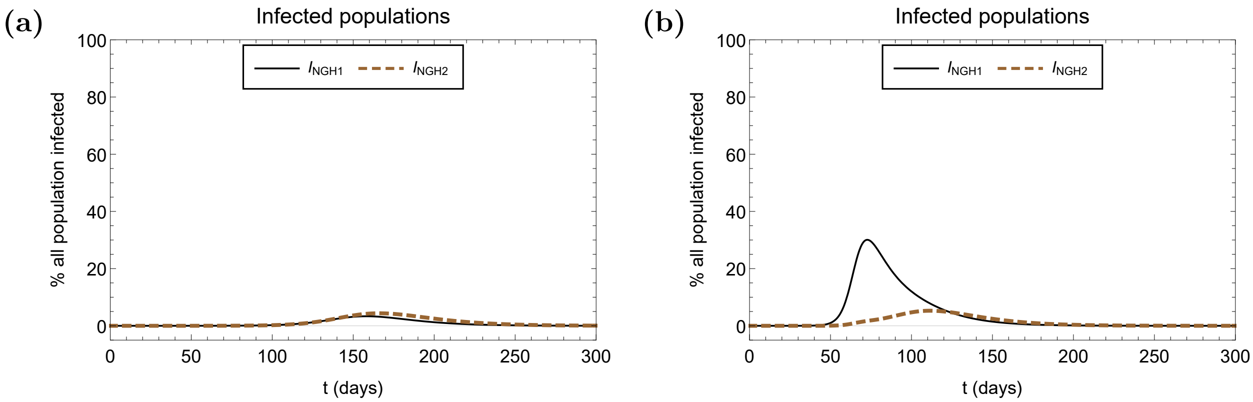

Figure 44: Total infections by neighborhood when the infection starts at HNN and transfers to HEN through commuter workers, with a) $\alpha_E = 0$, b) $\alpha_E = 1/24$. It is clear that changing α_E has negligible effect on the HNN, and an enormous impact on the HEN. If essential workers are allowed at non-essential locations for 1 h ($\alpha_E = 1$), the initial location of the disease becomes irrelevant, the HEN is always more heavily impacted than the HNN (compare Figures 40b and 44b).

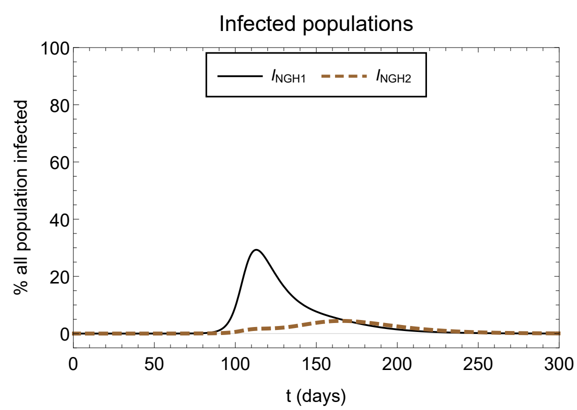

Figure 45: Total infections by neighborhood when the infection starts at HNN and transfers to HEN through commuter workers, with $\alpha_E = 0.01/24$. It is clear that, even for this small value of α_E, the effect on the HNN is negligible, and it is huge on the HEN. This means that population of an HEN are at a higher risk if lockdowns of essential workers at non-essential locations are not perfect (compare this result with Figure 44b).

5 Conclusions and Outlook

In this work, we proposed the LP-SIR, which is a modification of the classic SIR model that accounts for demographics in the form of "essential" (those that must interact face-to-face) and "non-essential" (those than can work from home) workers, and the behavioral response of the population to mask policies implemented by local governments to address an outbreak of an infectious disease. This model overcomes many limitations of the classic SIR model by adding features that account for heterogeneity in the population and enable a physical interpretation of the parameters in the model. For instance, time interaction parameters allow essential and non-essential workers to interact for different times (given as fractions of the daily time spent) at essential and non-essential businesses.

The distinction between cautious and risky workers and the division of locations into essential and non-essential businesses result in two types of dynamics. When interactions happen at non-essential locations, infections are slower for cautious individuals and faster for risky people. This may serve to explain the double peaks observed in infection curves for many states in the US. When interactions happen at essential locations, a homogeneous mixing is obtained due to the mask policy. In a real situation, there would be an averaging of these two situations, as interactions happen at both kind of locations.

By adding a further subdivision of essential and non-essential workers, it was possible to assess the effectiveness of mask mandates at essential locations and lockdown policies at non-essential locations. We found that mask usage can be effective in reducing the impacts of an outbreak by reducing contagions at essential locations, provided that facemasks are worn by almost all the population (mask compliance). We also found that lockdown policies at non-essential locations are particularly important for the non-essential risky population. This is especially important at the beginning of an outbreak as we showed that delays in implementing the policies fade out the potential benefits to slowdown or eradicate the infection.

The LP-SIR model predicts that essential workers have a central role in transmitting an infectious disease and suffer disproportionately from it. The results showed that they can act as reservoirs for the disease during periods in which lockdowns for non-essential workers are implemented. We also found that essential workers have a higher benefit than non-essential workers when compliance with mask mandates at essential locations is high. Given these findings, the role of essential workers should not be overlooked. Data that provides statistics for essential workers alone would allow to test some of these predictions. In case these findings are confirmed, testing essential workers may prove to be a viable strategy to contain the disease.

It must be emphasized that the LP-SIR model considers a series of simplifying assumptions that make the model computationally tractable. The most stringent assumption is that all compartments are considered as monolithic groups. This means that all individuals in a particular group behave homogeneously and have a rigid behavior towards policies. For instance, no risky individual interacts with a cautious one at non-essential locations. It also implies that all essential workers (or non-essential workers) behave and interact in the same way within a community, which is not strictly valid in a state due to the differences between urban and rural areas (e.g. when we applied the LP-SIR model to TX, NY and CA). That being said, there is always trade-off between the complexity of the model and the level of detail it includes. Our results suggest that the characteristics we chose to account for heterogeneities in the population are indeed important when deciding the set of policies to respond to an outbreak. Another limitation of our model is that it does not consider stochasticity. So, the LP-SIR model cannot account for effects that are statistical in nature, such as superspreaders or contagions, or within a family that may occur at home, with a specific set of individuals.

The LP-SIR model can be used to analyze transmission between heterogeneously composed communities. We found that the composition of a neighborhood may determine the outcome of an outbreak of an infectious disease. In particular, when analyzing two interacting neighborhoods, we found that essential workers commuting from one neighborhood to others play an important role as drivers of the disease. It was also found that the percentage of essential workers in a neighborhood determines the outcome of the infection. In neighborhoods with a prevalence of essential workers, the impact is higher than in neighborhoods where non-essential workers dominate, given that essential workers are allowed to interact at non-essential locations. Strikingly, this was always true except when they were completely locked out of non-essential locations, which is unrealistic since they move through non-essential locations to go to work.

As of this writing, vaccines for COVID-19 are available and they have helped to reduce or contain the spread in several countries. Their effect on the dynamics could, in principle, be included in the LP-SIR model. The only caveat is that a mindful choice of the parameters to add must be made. There are many different vaccines (with more to come), so modelling vaccine efficacy is a huge challenge on itself. There may also be a link between mask avoidance (risky behavior) and vaccine avoidance that is not easily modeled. A thorough consideration must be made between adding vaccination or working towards understanding the dynamics of a new disease. Both paths seem worthwhile at the moment, with variants of the COVID-19 disease still surrounding us and with the expectation of new and more resistant virus and bacteria to come (which increases the likelihood of new pandemics). This work focuses solely on the infection dynamics controllable solely via NPIs.

A potential research direction would be to determine the mobility of essential and non-essential workers from cellular and GPS databases by correlating the time spent at essential locations (determined by the GPS) to the type of worker, essential workers must spend their 8 h shift at essential locations. With this segregated data, predictions of the LP-SIR model can be better tested. In particular, it would become possible to determine with certainty if essential workers are exposed to a higher risk than non-essential workers. This may prove of great importance in determining the policies to contain an infectious disease, as one could do a targeted testing and quarantine/isolation of essential workers instead of focusing in the entire population.

More research is needed to determine the exact effect of compartmental sizes on the LP-SIR model. Since these values vary from one local community to others, it is paramount to fully understand the size effects onto the infection. One example of size effects affecting the dynamics is that if a community managed to reduce their percentage of risky people, then extended lockdowns could possibly be avoided.

Bibliography

[1] Kirsty R. Short, Katherine Kedzierska, and Carolien E. van de Sandt. "Back to the Future: Lessons Learned From the 1918 Influenza Pandemic". In: *Frontiers in Cellular and Infection Microbiology* 8.343 (Oct. 2018), pp. 1–19.

[2] John M. Barry. "The site of origin of the 1918 influenza pandemic and its public health implications". In: *Journal of Translational Medicine* 2.1 (Jan. 2004), pp. 1–4.

[3] Kristian G. Andersen et al. "The proximal origin of SARS-CoV-2". In: *Nature Medicine* 26.4 (Apr. 2020), pp. 450–452.

[4] Brian L. Hoffman. "Influenza activity in Saint Joseph, Missouri 1910-1923: Evidence for an early wave of the 1918 pandemic". In: *PLoS Currents* 2 (2011).

[5] B. J. Cowling et al. "Face masks to prevent transmission of influenza virus: a systematic review". In: *Epidemiology and Infection* 138.4 (Apr. 2010), pp. 449–456.

[6] Howard Markel et al. "Nonpharmaceutical interventions implemented by US cities during the 1918-1919 influenza pandemic". In: *Journal of the American Medical Association* 298.6 (Aug. 2007), pp. 644–654.

[7] Richard J. Hatchett, Carter E. Mecher, and Marc Lipsitch. "Public health interventions and epidemic intensity during the 1918 influenza pandemic". In: *Proceedings of the National Academy of Sciences of the United States of America* 104.18 (May 2007), pp. 7582–7587.

[8] Husch Blackwell. *State-by-State COVID-19 Guidance*. URL: `https://www.huschblackwell.com/state-by-state-covid-19-guidance`.

[9] Savannah Bergquist, Thomas Otten, and Nick Sarich. "COVID-19 pandemic in the United States". In: *Health Policy and Technology* 9.4 (Dec. 2020), pp. 623–638.

[10] Muhammad Farhan Bashir, Benjiang Ma, and Luqman Shahzad. "A brief review of socio-economic and environmental impact of Covid-19". In: *Air Quality, Atmosphere and Health* 13.12 (Dec. 2020), pp. 1403–1409.

[11] Jasper Verschuur, Elco E. Koks, and Jim W. Hall. "Global economic impacts of COVID-19 lockdown measures stand out in highfrequency shipping data". In: *PLoS ONE* 16.4 April (Apr. 2021), e0248818.

[12] The Institute for Health Metrics and Evaluation (IHME). *COVID-19 Data and Projections*. URL: `https://covid19.healthdata.org/global`.

[13] World Health Organization (WHO). *Severe Acute Respiratory Syndrome (SARS)*. URL: `https://www.who.int/health-topics/severe-acute-respiratory-syndrome#tab=tab_1`.

[14] Philip Ball. "The lightning-fast quest for COVID vaccines - and what it means for other diseases". In: *Nature* 589.7840 (Jan. 2021), pp. 16–18.

[15] Walter Dodds. "Disease Now and Potential Future Pandemics". In: *The World's Worst Problems*. Springer International Publishing, 2019, pp. 31–44.

[16] Rory Gibb et al. "Zoonotic host diversity increases in human-dominated ecosystems". In: *Nature* 584.7821 (Aug. 2020), pp. 398–402.

[17] David M. Morens and Anthony S. Fauci. "Emerging Pandemic Diseases: How We Got to COVID-19". In: *Cell* 182.5 (Sept. 2020), pp. 1077–1092.

[18] Long H Nguyen et al. "Risk of COVID-19 among front-line health-care workers and the general community: a prospective cohort study". In: *The Lancet Public Health* 5.9 (2020), pp. 475–483.

[19] Joanna Gaitens et al. "Covid-19 and essential workers: A narrative review of health outcomes and moral injury". In: *International Journal of Environmental Research and Public Health* 18.4 (Feb. 2021), pp. 1–16.

[20] W Kermack and A Mckendrick. "A contribution to the mathematical theory of epidemics". In: *Proceedings of the Royal Society of London. Series A, Containing Papers of a Mathematical and Physical Character* 115.772 (Aug. 1927), pp. 700–721.

[21] Fred Brauer, Pauline van den Driessche, and Jianhong Wu. *Mathematical Epidemiology.* Vol. 1945. Lecture Notes in Mathematics. Berlin, Heidelberg: Springer Berlin Heidelberg, 2008.

[22] Fred Brauer, Carlos Castillo-Chavez, and Zhilan Feng. *Mathematical Models in Epidemiology.* Vol. 69. Texts in Applied Mathematics. New York, NY: Springer New York, 2019.

[23] Centers for Disease Control and Prevention. *Interim Guidance on Duration of Isolation and Precautions for Adults with COVID-19.* URL: `https://www.cdc.gov/coronavirus/2019-ncov/hcp/duration-isolation.html`.

[24] Steffen E. Eikenberry et al. "To mask or not to mask: Modeling the potential for face mask use by the general public to curtail the COVID-19 pandemic". In: *Infectious Disease Modelling* 5 (Jan. 2020), pp. 293–308.

[25] Giulia Giordano et al. "Modelling the COVID-19 epidemic and implementation of population-wide interventions in Italy". In: *Nature Medicine* 26.6 (June 2020), pp. 855–860.

[26] Li Zhang et al. "Optimal parameterization of COVID-19 epidemic models". In: *Atmospheric and Oceanic Science Letters* 14.4 (Dec. 2021), p. 100024.

[27] Kian Boon Law et al. "Tracking the early depleting transmission dynamics of COVID-19 with a time-varying SIR model". In: *Scientific Reports* 10.1 (Dec. 2020), pp. 1–11.

[28] Fadoua Balabdaoui and Dirk Mohr. "Age-stratified discrete compartment model of the COVID-19 epidemic with application to Switzerland". In: *Scientific Reports* 10.1 (Dec. 2020), pp. 1–12.

[29] Rinaldo M. Colombo et al. "An age and space structured SIR model describing the Covid-19 pandemic". In: *Journal of Mathematics in Industry* 10.1 (Dec. 2020), pp. 1–20.

[30] Anca Rădulescu, Cassandra Williams, and Kieran Cavanagh. "Management strategies in a SEIR-type model of COVID 19 community spread". In: *Scientific Reports* 10.1 (Dec. 2020), pp. 1–16.

[31] Samuel Mwalili et al. "SEIR model for COVID-19 dynamics incorporating the environment and social distancing". In: *BMC Research Notes* 13:352.1 (July 2020), pp. 1–5.

[32] Calvin Tsay et al. "Modeling, state estimation, and optimal control for the US COVID-19 outbreak". In: *Scientific Reports* 10.1 (Dec. 2020), pp. 1–12.

[33] Lasko Basnarkov. "SEAIR Epidemic spreading model of COVID-19". In: *Chaos, Solitons and Fractals* 142 (Jan. 2021), p. 110394.

[34] Jeremy Howard et al. "An evidence review of face masks against COVID-19". In: *Proceedings of the National Academy of Sciences of the United States of America* 118.4 (Jan. 2021), e2014564118–.

[35] Neil M Ferguson et al. *Impact of non-pharmaceutical interventions (NPIs) to reduce COVID-19 mortality and healthcare demand*. Tech. rep. Imperial College London, 2020, pp. 1–20.

[36] Lee Worden et al. "Estimation of effects of contact tracing and mask adoption on COVID-19 transmission in San Francisco: a modeling study". In: *medRxiv : the preprint server for health sciences* (June 2020), p. 2020.06.09.20125831.

[37] Walmart Corporation. *Important Store Info. Store Hours*. URL: `https://corporate.walmart.com/important-store-info`.

[38] Office of the New York City Comptroller. *New York City's Frontline Workers*. URL: `https://comptroller.nyc.gov/reports/new-york-citys-frontline-workers/`.

[39] Legislative Analyst's Office (LAO) California. *COVID-19 and the Labor Market: Who Are California's Frontline and Remote Workers?* URL: `https://lao.ca.gov/LAOEconTax/Article/Detail/593`.

[40] Texas Workforce Commission. Labor Market and Career Information. *Labor Market and Career Information*. URL: `https://lmci.state.tx.us/shared/catalog.asp`.

[41] Apple. *COVID-19 - Mobility Trends Reports*. URL: `https://covid19.apple.com/mobility`.

[42] Google. *COVID-19 Community Mobility Reports*. URL: https://www.google.com/covid19/mobility/.

[43] M. Piraveenan, M. Prokopenko, and A. Y. Zomaya. “Local assortativity and growth of Internet”. In: *European Physical Journal B* 70.2 (July 2009), pp. 275–285.